Pergamon

Geochimica et Cosmochimica Acta, Vol. 66, No. 13, pp. 2399–2419, 2002

0016-7037/02 $22.00 + .00

PII S0016-7037(02)00831-1

Precise geochronology of phoscorites and carbonatites: The critical role of U-series disequilibrium in age interpretations

YURI AMELIN,[1,*] and ANATOLY N. ZAITSEV[2,3]

Geochronology Laboratory, Royal Ontario Museum, 100 Queen's Park, Toronto, ON M5S2C6,Canada
Institut fuer Mineralogie, Petrologie und Geochemie, Universitaet Freiburg, Albertstr. 23 b 79104 Freiburg, Germany
Department of Mineralogy, St. Petersburg State University, St. Petersburg 199034, Russia

(*Received December* 18, 2000; *accepted in revised form November* 6, 2001)

Abstract—We present the results of a comparative study of several geochronometer minerals (baddeleyite, zircon, apatite, phlogopite and tetraferriphlogopite) and isotopic systems (U-Pb, Th-Pb and Rb-Sr) from phoscorites (magnetite-forsterite-apatite-calcite rocks) and carbonatites of the Kovdor ultramafic-alkaline-carbonatite massif, Kola Peninsula, Russia. Uranium, thorium and their decay products are extremely fractionated by minerals that crystallise from carbonatite and phoscorite magma. We obtain high-precision ages from different chronometers, compare their accuracy, and evaluate the role of geochronological pitfalls of initial radioactive disequilibrium, differential migration of radiogenic isotopes, and inaccurate decay constants.

Apatite yielded concordant U-Th-Pb ages between 376 and 380 Ma. The accuracy of the apatite ^{238}U-^{206}Pb ages is, however, compromised by uncertainty in the amount of radiogenic ^{206}Pb produced from initial excess ^{230}Th. The ^{235}U-^{207}Pb ages are relatively imprecise due to large common Pb correction and the uncertainty in the initial Pb isotopic composition. The Th-Pb system yields a more precise age of 376.4 ± 0.6 Ma.

Zircon from two carbonatite samples is characterised by moderate to low U contents, high Th contents, and very high Th/U ratios up to 9000. The ^{206}Pb*/^{238}U systems in the zircon are strongly affected by the presence of excess ^{206}Pb*, produced by decay of initial ^{230}Th. The ^{208}Pb*/^{232}Th ages of zircon from both carbonatite samples are uniform and yield a weighted average of 377.52 ± 0.94 Ma.

Baddeleyite U-Pb analyses are 3 to 6% normally discordant and have variable ^{207}Pb*/^{206}Pb* apparent ages. Eleven alteration-free baddeleyite fractions from three samples with no evidence for Pb loss yield uniform ^{206}Pb*/^{238}U ages with a weighted average of 378.54±0.23 Ma (378.64 Ma after correction for initial ^{230}Th deficiency), which we consider the best estimate for age of the phoscorite-carbonatite body of the Kovdor massif. The ^{206}Pb*/^{238}U ages of baddeleyite fractions from five other samples spread between 378.5 and 373 Ma, indicating a variable lead loss up to 1.5%. The anomalously old ^{207}Pb/^{235}U and ^{207}Pb/^{206}Pb ages are consistent with the presence of excess radiogenic ^{207}Pb* in the baddeleyite. We interpret this as a result of preferential partitioning of ^{231}Pa to baddeleyite.

Fifteen phlogopite and tetraferriphlogopite fractions from five carbonatite and phoscorite samples yielded precise Rb-Sr isochron age of 372.2 ± 1.5 Ma, which is 5 to 7 m.y. younger than our best estimate based on U-Th-Pb age values. This difference is unlikely to be a result of the disturbance or late closure of Rb-Sr system in phlogopite, but rather suggests that the accepted decay constant of ^{87}Rb is too high.

Comparative study of multiple geochronometer minerals from the Kovdor massif has revealed an exceptional complexity of isotopic systems. Reliable ages can be understood through systematic analysis of possible sources of distortion. No single geochronometer is sufficiently reliable in these rocks. Th-Pb and Rb-Sr can be a very useful supplement to U-Pb geochronometry, but the routine use of these geochronometers together will require more precise and accurate determination of decay constants for ^{232}Th and ^{87}Rb. *Copyright © 2002 Elsevier Science Ltd*

1. INTRODUCTION

Recent progress in analytical techniques has greatly improved the precision of isotopic dating. This provides the potential to resolve geological events very close in time, e.g., crystallisation of individual phases in igneous complexes. On the other hand, the sources of error like uncertainty in decay constants, and effects caused by deviation from initial secular equilibrium, which were safely ignored at a lower precision of dating, become significant with improving precision and have to be accounted for. The first aim of this study is to explore these effects in a natural system—an alkaline-carbonatite igneous complex, in which extreme elemental fractionation both facilitates high precision dating, and enhances the initial disequilibrium.

Carbonatites and related alkaline and ultrabasic rocks are thought to be formed by deep-mantle plumes penetrating through continental lithosphere (e.g., Gerlach et al. 1988, Bell and Simonetti 1996, Bell 1998). The precision of 0.3 to 1.0 Ma is required for resolving individual pulses of magmatism, and for studying the dynamics of continental rifting and plume-lithosphere interaction, but the approach to precise and accurate dating of carbonatites and related rocks is not well established. The second aim of this study is to search for a precise and accurate way of dating carbonatites.

Carbonatites and phoscorites (magnetite-forsterite-apatite-

* Author to whom correspondence should be addressed (yuria@rom.on.can).

calcite rocks) contain numerous minerals enriched in U and(or) Th: baddeleyite, zircon, apatite, zirconolite, perovskite, pyrochlore. It may seem therefore that precise age determination of these rocks using the U-Pb method is easy and straightforward. However, enrichment in U, Th and their decay products also causes deviation from the secular radioactive equilibrium in growing minerals, which results over time in the excess or deficiency of radiogenic Pb isotopes. To optimise approach to high-precision dating of carbonatites and phoscorites, and to assure the accuracy of ages, a number of questions need to be answered:

- Are the isotopic data of coexisting mineral chronometers consistent with each other? Which mineral chronometers are more reliable?
- How consistent are the U-Pb and Th-Pb ages?
- To what extent are the U-Pb ages affected by initial isotopic disequilibrium in uranium decay chains?
- Are the data obtained by U-Pb method compatible with the results of Rb-Sr dating, previously widely used for dating carbonatite complexes?

We explore these questions in a detailed study of potential mineral geochronometers from phoscorites and carbonatites of the Kovdor massif, an ultrabasic-alkaline-carbonatite massif in the Palaeozoic Kola Alkaline Province. The Kovdor massif contains wide compositional range of magmatic and metasomatic rocks, including several generations of carbonatites and phoscorites, and has not experienced regional metamorphism or deformation. The geology of the massif, including relative chronology of igneous phases, has been studied in detail, as well as petrology, mineralogy, mineral chemistry, major and trace element geochemistry, and isotope geochemistry (references in Zaitsev and Bell, 1995). In addition, the carbonatites and phoscorites of the Kovdor massif contain ubiquitous baddeleyite, apatite, phlogopite and tetraferriphlogopite, and in some carbonatites abundant zircon. Finally, accessory minerals from the Kovdor carbonatites and phoscorites are known to have highly fractionated ratios of trace elements with similar geochemical properties (e.g., Zr/Hf and Nb/Ta). These features together make the Kovdor massif an excellent choice for a comparative study of several potentially useful U-Pb, Th-Pb, and Rb-Sr chronometers.

2. GEOLOGY AND MINERAL PARAGENESIS

The Kovdor massif, with ca. 40.5 km^2 surface area, is a part of the Palaeozoic Kola Alkaline Province, which consists of more than twenty-four intrusive complexes of Devonian age (Kramm et al., 1993). The Kovdor massif is a typical ultrabasic-alkaline complex bearing a wide compositional range of magmatic and metasomatic rocks, including olivinite, pyroxenite, ijolite- melteigite, turjaite, melilitolite and various phoscorites and carbonatites. Kovdor is extremely important economically, with magnetite, apatite, baddeleyite, phlogopite and vermiculite as the main industrial targets, and has been the subject of detailed geological and mineralogical study by Russian geologists. General geology, petrography and mineralogy of the phoscorite and carbonatite occurrence in Kovdor have been described in numerous publications (e.g., Kukharenko et al., 1965; Kapustin, 1980; Krasnova & Kopylova, 1988).

Phoscorites and carbonatites occur at the contact of the pyroxenite and the ijolite intrusions in the south-western part of the massif (Fig. 1). They form a stockwork occur as steeply dipping veins and pipe-like, almost vertical bodies, which have been traced in drill holes to a depth of 1.5 km.

The phoscorites have a variable mineralogy, the major minerals being magnetite, forsterite, apatite, phlogopite, tetraferriphlogopite, calcite and dolomite. Petrographically the bodies are concentrically zoned. Their assemblages gradually change from forsterite and apatite-forsterite phoscorites at the rim, through apatite-forsterite-magnetite and phlogopite-calcite-forsterite-magnetite to a core of tetraferriphlogopite-calcite-forsterite-magnetite and dolomite-magnetite phoscorites (Fig. 2).

The carbonatites at Kovdor are represented by calcite and dolomite varieties. Mineral assemblages in carbonatites are similar to those in phoscorites, but with major carbonates. Several stages of phoscorite and carbonatite formation have been recognised at Kovdor on the basis of cross-cutting field relationships and mineralogy (Krasnova and Kopylova 1988). Both phoscorites and carbonatites contain several Nb-, Ta-, Zr-, Th and U-rich accessory minerals including zirconolite, calzirtite, pyrochlore, baddeleyite, zircon and perovskite. The crystallisation sequence and relationships of such minerals in carbonatites have been discussed by Kapustin (1980); Bulakh and Ivanikov (1984) and Williams (1996).

Previous geochronological study of the Kovdor massif have yielded Rb-Sr mineral ages of olivinite and pyroxenite of 376.1 $\pm$ 0.6 Ma, 374.3 $\pm$ 0.3 Ma, and 373.1 $\pm$ 4.6 Ma (U. Kramm, personal communication 1994), within the range of Rb-Sr ages of 380 to 360 Ma for the other intrusions in the Kola Alkaline Province (Kramm et al. 1993). U-Pb dating of baddeleyite from the Kovdor carbonatite and phoscorite yielded an age of 380 $\pm$ 4 Ma (Bayanova et al. 1991), later revised to 382 $\pm$ 3 Ma (Bayanova et al. 1997). An attempt of ^{39}Ar-^{40}Ar dating of nepheline produced apparent ages between 400 to 600 Ma (Karpenko and Ivanenko 1994), indicative of the presence of excess ^{40}Ar.

Isotopic data for the Kovdor carbonatites were first obtained as a part of a reconnaissance Sr-Nd isotopic study of the Kola Alkaline Province (Kramm 1993). Sr-Nd study of apatite, calcite and dolomite from phoscorites and carbonatites revealed two isotopically distinct groups of these rocks (Zaitsev and Bell 1995). Isotopic (Sr-Nd) and geochemical studies of Kovdor silicate rocks suggest a complex evolution with several magma batches derived from either a heterogeneous mantle source, or from variable proportion of mixing between two magma reservoirs (Verhulst et al. 2000). The noble gas and nitrogen isotope studies (Marty et al. 1998, Dauphas and Marty 1999) point to the origin of the Kovdor carbonatite magmas from a deep mantle plume.

3. SAMPLES

Fourteen representative samples from the main phases of phoscorites and carbonatites at Kovdor were analysed for this study. Table 1 presents the various stages and temporal relation of the phoscorites and carbonatites at Kovdor. The mineralogy of samples and the succession of phases based on geological relationships are also shown in Table 1. Eight out of the 14

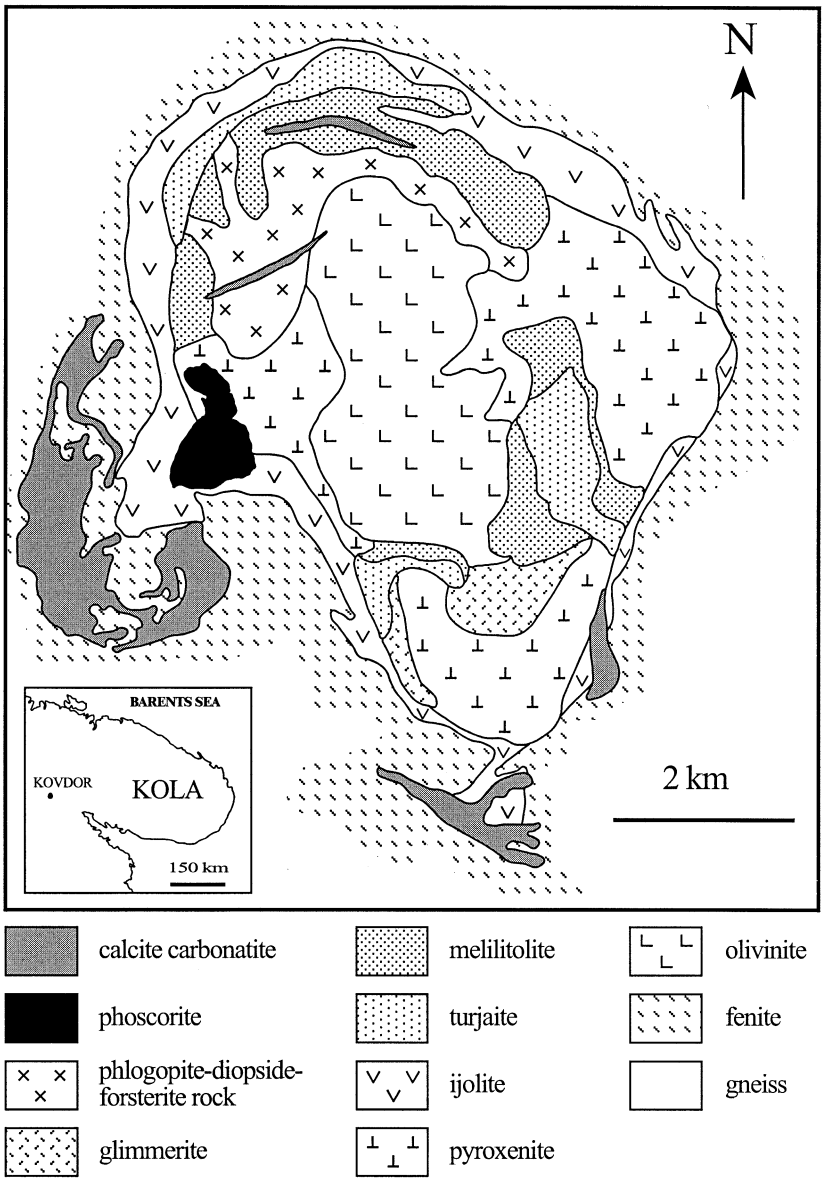

Fig. 1. Simplified geological map of the Kovdor massif, showing positions of phoscorites and carbonatites (after Kukharenko et al. 1965).

samples have been previously analysed for Rb-Sr and Sm-Nd (Zaitsev and Bell 1995).

4. ANALYTICAL TECHNIQUES

Minerals have been separated using standard heavy liquid and magnetic techniques, and hand-picked under a binocular microscope to produce 100% pure fractions of clear mineral grains or fragments, free of alteration, inclusions, and cracks (unless otherwise indicated in the tables). Some of the zircon and baddeleyite fractions were abraded (Krogh 1982). Before digestion, zircon was washed in 4N HNO_3 for 30 min on a hot plate with 100°C surface temperature (maximum temperature of the acids was ~60°C). Baddeleyite was washed in 2N HNO_3 in the same conditions. Mica was washed for 30 min in 2N HCl with ultrasonic agitation, to dissolve the adhering calcite and apatite. Calcite and apatite are readily soluble in HCl and HNO_3, and were therefore cleaned in milder conditions, by a brief (ca. 1 min) ultrasonic agitation in 0.1N HCl at room temperature, to remove possibly contaminated surface layer.

The U-Pb procedure generally follows those described by Amelin et al. (1994) and Amelin et al. (1997a) for analyses performed at the Royal Ontario Museum (ROM) and at the Washington University (WU). The main differences from the published procedures are related to the separation and isotopic analysis of Th, and to the use of several U-Pb and U-Th-Pb spikes during the various stages of this study. In the procedure that we used originally, the dissolved samples in 1N HBr were loaded on anionite (AG1 × 8) columns. Bulk fraction contain-

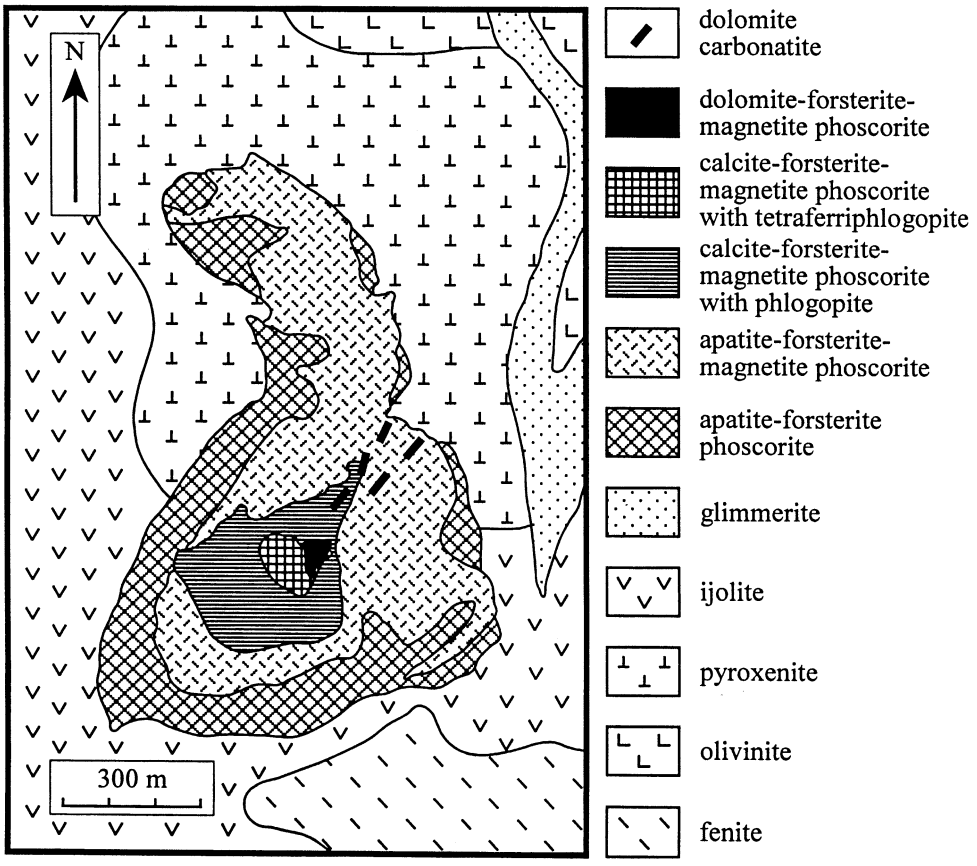

Fig. 2. Geological relationships within the phoscorite-carbonatite body (after Ternovoi 1977, Dunaev 1982). More detailed map of the phoscorite-carbonatite body has been presented by Krasnova and Kopylova (1988).

ing Th and U was collected as the HBr wash, and Pb was further eluted with 6N HCl. The Th and U separation using the same anionite columns with absorption from 7N HNO_3 and desorption in 6N HCl and H_2O was adopted from Tatsumoto (1966). The above procedure was used to analyse all apatite and some of the zircon and baddeleyite fractions. The total blanks were 5 ± 2 pg Pb, 0.2 ± 0.1 pg U. Since zircon and baddeleyite have very low Fe contents, and separation of Fe is therefore not required, we have adapted a version of the chemical separation procedure of Krogh (1973) in HCl media, modified for Th-U-Pb separation. This procedure uses smaller amount of HCl and no HBr, so we hoped to achieve lower Pb blank. In this case, samples were loaded on Bio-Rad AG1 $\times$ 8 anionite columns in 3.1N HCl. Bulk fractions containing Zr, Th and other elements were collected in 3.1N HCl wash. Pb and U, which are retained by the resin in 3.1 HCl, were extracted with 6N HCl and H_2O, respectively. Thorium was separated on the same columns using 7N HNO_3 and 6N HCl. This procedure yields a marginally lower blank of 3 ± 1.5 pg for Pb, and was used for zircon and baddeleyite analyses at the later stage of this study.

Isotopic analyses of Th were performed on a VG-354 mass spectrometer at the ROM in single collector mode, using various loading techniques. At the early stage, Th was loaded with silica gel on Re single filaments and analysed as ThO^+. This technique yields very low loading blank (below detection limit of $\sim$0.1 pg), but the ionisation efficiency and running conditions were not sufficiently reproducible. Later we accommo-

Table 1. Successive stages of formation of phoscorites and carbonatities of the Kovdor massif.

Stage	Phoscorite type Samples	Carbonatite type Samples
Ia	Forsterite, apatite-forsterite (Ph 1) KV-2, KV-3	
Ib	Apatite-forsterite-magnetite (Ph 2) KV-4	
Ic	Calcite-forsterite-magnetite with phlogopite (Ph 3) KV-5, KV-6, KV-8, KV-9	Calcite with forsterite and phlogopite (C 1) 1/84, KV-18, KV-25,
IIa	Calcite-forsterite-magnetite with tetraferriphlogopite (Ph 4)	Calcite with tetraferriphlogopite (C 2) KV-21, 244/76, 127/85
IIb	Dolomite-forsterite-magnetite, dolomite-magnetite (Ph 5)	Dolomite (C 3) 115/85

Based on the data of Krasnova & Kopylova (1988), stage division modified from Zaitsev & Bell (1995).

dated loading Th on a single Re filament between two layers of colloidal graphite (Edwards et al. 1986) and analysing as Th^+. This technique enhances Th emission from the filament metal, producing the $^{232}Th^+$ currents of $3*10^2$ to $2*10^3$ ions/s from graphite coated filaments without sample. However, these currents are insignificant compared to the ion beam produced by the samples, and the reproducibility of running conditions is far better than with the silica gel loads. The fractionation was checked by repeated runs of an internal Th isotopic standard prepared by mixing of natural Th and ^{230}Th spike. The $^{232}Th/^{230}Th$ ratio of 4.3611 ± 29 (95% conf.) in this standard was established by repeated total sample evaporation analyses. In addition, both loading techniques were used for Th analyses during spike calibration, and yielded compatible results.

Three different mixed spikes were used for U-Pb and U-Th-Pb analyses during this study: a ^{235}U-^{205}Pb spike previously used for U-Pb dating at the ROM, a ^{235}U-^{205}Pb spike with slightly different $^{235}U/^{205}$Pb ratio prepared for the U-Pb geochronological work at the WU, and a new ^{235}U-^{230}Th-^{205}Pb spike prepared at the ROM. In addition, a ^{229}Th-^{233}U-^{236}U-^{205}Pb spike for combined U-Pb and ^{230}Th-U dating was prepared at the ROM later (Neymark et al. 2000). All these four spikes were calibrated against the same set of four normal solutions. Three of these normal solutions were prepared of pure metals uranium SRM-960, and lead SRM-981 or SRM-982 at the ROM. The fourth normal solution was prepared of SRM-960 U, SRM-982 Pb, and a high purity Th metal at the NERC Isotope Geosciences Laboratory, Nottingham, by R.R. Parrish. The U/Pb ratios in the spikes measured against all four normal solutions agree within 0.1%. Further procedure check was done using two standard zircons, and the results are reported below.

Common Pb corrections were done by applying the Pb isotopic composition of low-U calcite from the same samples. For the samples from which no calcite has been analysed the correction used Pb isotopic composition of calcite from the phoscorite KV-5, the most primitive Pb found in Kovdor. Uncertainties of individual analyses were propagated using the PBDAT program version 1.24 (Ludwig 1993); errors are reported at 2σ .

Rb-Sr analyses follow the procedure of Amelin et al. (1997b). The two modifications are the use of the ^{85}Rb-^{84}Sr spike with higher $^{85}Rb/^{84}Sr = 912$, instead of the spike with $^{85}Rb/^{84}Sr = 9.83$ used in our previous Sr isotopic work, and a smaller size of the ion exchange columns used for the chemical separation of Rb and Sr. Both spikes were calibrated against the same mixed normal solution. Average procedure blanks were <0.7 pg Rb and 5 ± 2 pg Sr. One of the main sources of errors in Rb-Sr dating of minerals with high Rb/Sr ratios is the variable fractionation of Rb isotopes during analysis. The reproducibility of Rb isotopic fractionation varies substantially between ionisation methods. Loading Rb on Re filaments with silica gel (following Papanastassiou and Wasserburg 1971) resulted in ~2 to 2.5 times smaller range of fractionation than the two alternative methods: single oxidised Ta filaments, and triple filament assemblages. The average measured $^{85}Rb/^{87}Rb$ in our in-house natural Rb standard (a crystal of muscovite processed through our standard chemical procedure), loaded with silica gel, was 2.6163 ± 0.0040 (0.151%, 2 sd) for single Faraday collector runs, and 2.6316 ± 0.0117 (0.445%, 2 sd) for single Daly detector runs. These values were used for Rb fractionation correction, with appropriate error magnification, of analyses of the Kovdor micas and the standard feldspar. The Rb-Sr procedure was additionally checked by replicate analyses of the standard feldspar SRM-607, the results of which are discussed below.

Isochron, discordia line and weighted mean calculations were performed using the ISOPLOT program version 2.95 (Ludwig 1997). Errors of the ages are quoted at the 95% confidence level. Ages presented in the Tables 2–5 are calculated using the decay constants recommended by Steiger and Jager (1977).

5. RESULTS

5.1. Standard Zircon

U-Pb and Th-Pb results for the zircon standards 91500 and 61.308B are presented in Tables 2 and 3. The data for the zircon standard 91500 are also shown in Figure 3. Analyses of the zircon standard 91500 during certification (Wiedenbeck et al. 1995) showed variations in $^{206}Pb/^{238}U$ age with the total range of ca. 0.4%. These variations exceed analytical error and presumably result from recent Pb loss. Our $^{206}Pb/^{238}U$ data show a similar range of variations, but the fractions that we have analysed are substantially smaller than those of (Wiedenbeck et al. 1995) and the uncertainties are accordingly larger, so our data are consistent within error. The discordance of our analyses is slightly larger than those of Wiedenbeck et al. (1995). The difference between our $^{206}Pb/^{238}U$ weighted mean of 0.17867 ± 37 and the certified value of 0.17916 ± 20 (recalculated from Wiedenbeck et al. (1995) using ISOPLOT, error is 95% confidence interval) is ~0.25%. If this difference is considered real, it is not a result of a bias in spike calibration, because some of the measurements included in the compilation of Wiedenbeck et al. (1995) were done at the ROM using one of the spikes that were also used in this study. We rather attribute it to a slightly variable degree of Pb loss between zircon fragments, as was already pointed out by Wiedenbeck et al. (1995). Our three $^{208}Pb/^{232}Th$ analyses are also reproducible, and their weighted mean is well within error with the data of Wiedenbeck et al. (1995). The $^{207}Pb/^{206}Pb$ data are in excellent agreement with the certified values.

Our U-Th-Pb data for the zircon standard 91500 are thus similar in precision and accuracy to those obtained during certification. The only significant deviation is the low U/Pb ages of fraction 54, which has $^{208}Pb/^{232}Th$ and $^{207}Pb/^{206}Pb$ indistinguishable from other fractions. This points to a problem with U analysis, rather than normal discordance. In the past, we occasionally experienced high and variable U blank (up to 100 to 200 pg for the columns with 1 mL of resin) while using anionite resin stored in the lab for over 6 to 8 months. The problem was taken under control by washing anion exchange columns with HNO_3 (Amelin et al. 1997b). The fraction 54 was analysed before the HNO_3 washing was implemented as a mandatory part of the procedure, and was presumably affected by U excess from the resin. All the other analyses in this study were done using columns precleaned with HNO_3, with regular blank measurements confirming the negligible level of uranium contamination.

Table 2. Baddeleyite and zircon U-Pb data.

Fraction number	Sample 1)	Fraction 2)	Spike 3)	Fraction wt, mg	U ppm	Com.Pb pg 4)	Atomic ratios 6) 206/204 5)	206Pb/ 238U	2σ%err	207Pb/ 235U	2σ%err	207Pb/ 206Pb	2σ%err	Apparent age, Ma 206Pb/ 238U	2σ err	207Pb/ 235U	2σ err	207Pb/ 206Pb	2σ err	Discord %
Kovdor Complex																				
1	1/84	B col (30)	UPb	0.416	100	207	778	0.06023	0.202	0.45356	0.316	0.05461	0.196	377.05	0.76	379.77	1.20	396.41	4.40	4.88
2		B col (25)	UPb	0.407	96	166	917	0.06063	0.210	0.45596	0.324	0.05454	0.210	377.05	0.79	378.77	1.23	396.41	4.60	4.88
3		B col (1)	UPb	0.025	21	9.5	232	0.05998	0.486	0.44926	2.074	0.05432	1.938	375.52	1.83	376.76	7.81	384.37	43.20	2.30
4	244/76	B pb (32)	UPb	0.774	64	20.8	9,079	0.06030	0.206	0.45356	0.258	0.05455	0.150	377.47	0.78	379.77	0.98	393.80	3.40	4.15
5		B pb (18)	UPb	0.224	77	10.3	6,393	0.06036	0.332	0.45429	0.358	0.05458	0.184	377.84	1.25	380.28	1.36	395.15	4.20	4.38
6		B pb (9)	UPb	0.245	94	23.1	3,762	0.06016	0.338	0.45223	0.374	0.05451	0.176	376.62	1.27	378.84	1.42	392.38	4.00	4.02
7		B blk (41)	UPb	1.042	909	161	20,917	0.05668	0.762	0.42332	0.772	0.05417	0.098	355.41	2.71	358.42	2.77	378.00	2.20	5.98
8		B db (40)	UPb	1.060	71	20.5	13,822	0.06008	0.212	0.45203	0.250	0.05457	0.094	376.11	0.80	378.70	0.95	394.57	2.00	4.68
9		B pb (1) abr	UPb	0.007	37	2.5	414	0.06050	0.594	0.45332	3.430	0.05434	3.382	378.69	2.25	379.60	13.02	385.21	72.80	1.69
10		B pb (1) abr	UPb	0.010	25	9.8	116	0.06082	0.588	0.46352	3.642	0.05527	3.480	380.62	2.24	386.70	14.08	423.27	76.60	10.08
11		B pb (1) abr	UPb	0.011	64	1.7	1,607	0.06073	0.470	0.45808	1.190	0.05470	1.070	380.08	1.79	382.92	4.56	400.12	23.80	5.01
12		B pb (1) abr	UPb	0.011	127	1.4	3,885	0.06046	0.432	0.45712	0.620	0.05483	0.446	378.45	1.63	382.25	2.37	405.36	10.00	6.64
13	KV-3	B br (1)	UPbWU	1.455	131	29.8	25,182	0.06065	0.168	0.45612	0.188	0.05455	0.050	379.55	0.64	381.56	0.72	393.76	1.20	3.61
14		B br (1)	UThPb	0.209	30	10.3	2,334	0.06059	0.448	0.45649	0.474	0.05464	0.150	379.23	1.70	381.81	1.81	397.50	3.40	4.60
15		B br (1)	UThPb	0.280	89	7.8	11,968	0.05970	0.220	0.44905	0.228	0.05455	0.053	373.81	0.82	376.61	0.86	393.89	1.20	5.10
16		B pb (20) inc	UThPb	1.992	38	25.0	11,328	0.06012	0.176	0.45201	0.181	0.05453	0.042	376.33	0.66	378.69	0.68	393.13	0.94	4.27
17		B br (20) euh	UThPb	1.920	76	36.0	15,395	0.06028	0.168	0.45350	0.172	0.05456	0.039	377.35	0.63	379.72	0.65	394.21	0.86	4.28
18	KV-4	B br (8)	UpbWU	0.966	92	27.6	12,476	0.05963	0.160	0.44832	0.194	0.05453	0.058	373.39	0.60	376.10	0.73	392.85	1.20	4.95
19		B br (3)	UpbWU	0.560	64	28.3	4,920	0.06012	0.286	0.45186	0.356	0.05451	0.100	376.35	1.08	378.58	1.35	392.26	2.20	4.06
20		B pb (12)	UThPb	0.752	80	20.0	11,618	0.05959	0.218	0.44815	0.226	0.05454	0.063	373.13	0.81	375.98	0.85	393.60	1.40	5.20
21		B br (18)	UThPb	0.792	94	22.0	12,956	0.06005	0.232	0.45113	0.240	0.05449	0.061	375.91	0.87	378.07	0.91	391.33	1.36	3.94
22	KV-5	B br (1)	UPbWU	0.616	71	7.9	20,823	0.06043	0.476	0.45468	0.476	0.05457	0.136	378.22	1.80	380.55	1.81	394.76	3.00	4.19
23		B br (1) long	UPbWU	0.225	113	5.5	17,589	0.06049	0.216	0.45461	0.224	0.05451	0.092	378.58	0.82	380.50	0.85	392.18	2.00	3.47
24		B br (1)	UPbWU	0.167	158	12.7	7,874	0.06036	0.284	0.45357	0.284	0.05450	0.180	377.82	1.07	379.78	1.08	391.74	4.00	3.55
25		B br (1)	UPbWU	1.286	48	11.0	21,816	0.06046	0.136	0.45393	0.158	0.54450	0.054	378.44	0.51	380.03	0.60	389.69	1.20	2.89
26		B br (10) euh	UThPb	1.754	91	18.0	34,629	0.06054	0.208	0.45475	0.212	0.05448	0.040	378.89	0.79	380.60	0.81	391.00	0.90	3.10
27		B br (4) euh	UThPb	1.797	69	26.0	18,270	0.06056	0.172	0.45480	0.178	0.05446	0.044	379.06	0.65	380.64	0.68	390.26	0.98	2.87
28	KV-6	B br (1)	UPbWU	0.216	154	6.7	19,118	0.05966	0.210	0.44861	0.230	0.05454	0.080	373.54	0.78	376.31	0.87	393.36	1.80	5.04
29		B db (4)	UPbWU	0.608	191	9.7	46,635	0.06060	0.160	0.45599	0.176	0.05457	0.046	379.27	0.61	381.47	0.67	394.81	1.00	3.94
30		B br (5) euh	UPb	0.381	133	6.1	31,438	0.06037	0.310	0.45474	0.338	0.05463	0.084	377.85	1.17	380.59	1.29	397.31	1.80	4.90
31		B db (1) euh	UPb	0.302	128	5.2	27,773	0.05978	0.420	0.45071	0.440	0.05468	0.104	374.26	1.57	377.78	1.66	399.36	2.20	6.29
32		B db (1)	UThPb	0.266	148	6.3	23,807	0.05989	0.548	0.45046	0.550	0.05455	0.054	374.96	2.05	377.60	2.08	393.79	1.22	4.78
33		B db (1)	UThPb	0.318	147	5.8	30,553	0.06057	0.276	0.45609	0.280	0.05461	0.047	379.09	1.05	381.54	1.07	396.43	1.06	4.37
34		B br (7)	UThPb	0.851	145	8.2	57,081	0.06023	0.185	0.45338	0.192	0.05459	0.053	377.03	0.70	379.64	0.73	395.63	1.30	4.70
35		B db (5) euh	UThPb	0.843	166	5.5	97,032	0.06046	0.190	0.45529	0.195	0.05462	0.044	378.42	0.72	380.98	0.74	396.57	0.98	4.58
36	KV-8	B db (2)	UPbWU	0.527	73	15.3	9,808	0.06052	0.186	0.45485	0.206	0.05451	0.072	378.79	0.70	380.67	0.78	392.14	1.60	3.40
37		Ba pb (10)	UPbWU	1.186	54	29.7	8,423	0.06042	0.208	0.45388	0.252	0.05448	0.074	378.18	0.79	379.99	0.96	391.08	1.60	3.30
38	KV-9	B br (1) inc	UPbWU	0.268	53	7.7	7,000	0.06044	0.338	0.45518	0.356	0.05462	0.182	378.28	1.28	380.90	1.36	396.87	4.00	4.68

(Continued)

Table 2. (Continued)

Fraction number	Sample 1)	Fraction 2)	Spike 3)	Fraction wt, mg	U ppm	Com.Pb pg 4)	Atomic ratios 6) 206/204 5)	206Pb/ 238U	2σ %err	207Pb/ 235U	2σ %err	207Pb/ 206Pb	2σ %err	Apparent age, Ma 206Pb/ 238U	2σ %err	207Pb/ 238U	2σ err	207Pb/ 206Pb	2σ err	Discord %
39		B br (1)	UPbWU	0.278	139	4.4	33,345	0.06039	0.202	0.45403	0.212	0.05453	0.072	377.98	0.76	380.10	0.81	393.01	1.60	3.82
40		B br (1) long	UPbWU	0.166	93	6.6	8,835	0.06052	0.198	0.45507	0.226	0.05453	0.108	378.80	0.75	380.83	0.86	393.15	2.40	3.65
41	115/85	Z br (1) abr	UPb	0.132	0.21	1.0	179.0	0.09485	2.792	0.45233	20.306	0.03459	19.812	584.17	16.31	378.91	76.94			
42		Z br (6) abr	UPb	0.351	0.08	1.4	237.0	0.16374	37.554	0.41624	93.458	0.01844	83.200	977.51	367.09	353.36	330.24			
43		Z yel (1) abr	UPb	0.128	0.15	1.0	184.0	0.13868	3.636	0.35366	76.938	0.01850	74.924	837.21	30.44	307.47	236.56			
44		Z yel (7) abr	UPb	0.381	0.06	8.4	39.8	0.10312	2.898	0.48815	58.268	0.03433	56.264	632.67	18.33	403.65	235.20			
45		Z br (10) abr	UThPb	0.984	0.13	2.5	317.2	0.09392	17.620	0.23320	19.620	0.01801	8.460	578.70	101.97	212.83	41.76			
46		Z yel (10) abr	UThPb	0.866	0.09	3.1	163.1	0.09260	28.600	0.54666	37.800	0.04282	23.600	570.89	163.27	442.80	167.38			
47		Z col (10) abr	UThPb	0.709	0.10	2.1	208.3	0.08762	30.800	0.40823	32.000	0.03379	8.180	541.47	166.77	347.60	111.23			
48	127/85	Z br (4) fib abr	UPb	0.472	43	9.1	8,288	0.05883	0.248	0.43563	0.280	0.05371	0.126	368.50	0.91	367.17	1.03	358.73	2.80	−2.72
49		Z br (4) fib abr	UThPb	0.169	52	3.4	8,423	0.05209	0.398	0.38942	0.420	0.05422	0.132	327.34	1.30	333.95	1.40	380.24	3.00	13.91
50		Z pb (6) abr	UThPb	0.145	36	3.5	5,506	0.05876	0.548	0.43771	0.576	0.05400	0.175	368.63	2.02	368.63	2.12	371.11	4.00	0.77
51		Z br (3) fib abr	UThPb	0.392	35	4.9	10,278	0.05906	0.364	0.43908	0.378	0.05392	0.102	369.89	1.35	369.61	1.40	367.85	2.20	−0.55
52		Z br (12) fib abr	UThPb	1.045	39	3.9	38,601	0.05919	0.208	0.43856	0.214	0.05374	0.050	370.68	0.77	369.23	0.79	360.20	1.14	−2.91
53		Z br (9) fib	UThPb	0.576	53	4.6	21,397	0.05182	0.232	0.37593	0.246	0.05261	0.082	325.70	0.76	324.04	0.80	312.15	1.86	−4.34
Zircon standards																				
54	91500	Z	UThPb	0.076	75	3.4	18,427	0.17727	0.391	1.83126	0.398	0.07492	0.096	1052.10	4.11	1056.70	4.21	1066.40	1.40	1.34
55		Z	UThPb	0.459	84	5.7	74,324	0.17914	0.393	1.84920	0.396	0.07487	0.049	1062.30	4.17	1063.10	4.21	1065.00	0.99	0.25
56		Z	UUThPb	0.031	76	1.3	20,068	0.17888	0.302	1.84622	0.314	0.07486	0.086	1060.80	3.20	1062.10	3.33	1064.60	1.70	0.36
57		Z	UUThPb	0.042	73	0.9	36,504	0.17915	0.342	1.85029	0.400	0.07491	0.207	1062.30	3.63	1063.50	4.25	1066.00	4.20	0.35
58		Z	UUThPb	0.012	83	0.9	12,259	0.17822	0.349	1.83827	0.365	0.07481	0.106	1057.20	3.69	1059.20	3.87	1063.40	2.10	0.58
59		Z	UUThPb	0.177	79	13.5	10,421	0.17813	0.371	1.83885	0.382	0.07487	0.086	1056.70	3.92	1059.40	4.05	1065.00	1.70	0.78
60		Z	UUThPb	0.177	79	3.6	42,168	0.17827	0.360	1.84109	0.365	0.07490	0.060	1057.50	3.81	1060.20	3.87	1065.90	1.20	0.79
61		Z	UPb	0.177	67	2.3	55,024	0.17883	0.206	1.84706	0.213	0.07491	0.055	1060.60	2.18	1062.40	2.26	1066.10	1.10	0.52
		Certified 7)			81			0.17916	0.112	1.85020	0.092	0.07488	0.027	1062.40	1.19	1063.50	0.98	1065.43	0.57	0.28
62	61.308B	Z	UUThPb	0.171	183	15.0	61.2	0.000390	8.16	0.002833	22.50	0.05266	18.90	2.514	0.205	2.872	0.646	314	430	
63		Z	UUThPb	0.171	166	3.1	239.1	0.000389	5.27	0.002832	9.35	0.05284	7.31	2.505	0.132	2.872	0.268	322	170	
64		Z	UPb	0.171	145	8.1	97.4	0.000380	6.49	0.002774	12.60	0.05286	10.30	2.452	0.159	2.813	0.354	324	230	
		Certified 7)			218			0.000389	0.13	0.002773	1.20	0.05161	0.94	2.501	0.003	2.810	0.034	270	27	

1) Rock names and intrusive phases are indicated in Table 1. 2) fraction: B-baddeleyite, Z-zircon, col-colorless, pb-pale brown, br-brown, db-dark brown, blk-black, yel-yellow arb-abraded, euh-euhedral, inc-opaque inclusions, fib-fiber-shaped grayish inclusions. 3) Spike: UPb-235U-205Pb spike (ROM); UThPb-235U-230Th-205Pb spike (ROM); UUThPb-233U-236U-229Th-205Pb spike (ROM); UPbWU-235-205Pb spike (Washington University). 4) total common Pb in fraction. 5) The 206Pb/204Pb ratios are corrected for spike and fractionation, but not for procedure blank. 6) Atomic ratios corrected for blank, spike, fractionation and initial common Pb.

Table 3. Th-Pb data.

Fraction number 1)	Sample	Fraction	Fraction wt, mg	U ppm	Th ppm	Th/U	Atomic ratios 2) 208Pb/ 204Pb	2σ% err	232Th/ 204Pb	2σ% err	208Pb*/ 232Th	2σ% err	208Pb*/ 232Th Age, Ma 3)	2σ err
66	KV-2	Ap	9.027	2.489	57.77	23.21	139.6	0.17	5,366	0.38	0.018885	0.43	378.16	1.41
14	KV-3	B	0.209	29.85	1.617	0.054	84	42.4	3,029	67.0	0.021269	3.30	425.38	14.04
15		B	0.280	88.86	5.984	0.067	260	91.4	22,690	101	0.015951	0.85	319.86	2.71
16		B	1.992	37.87	3.364	0.089	348	27.6	20,550	30.4	0.017957	0.37	359.73	1.35
17		B	1.920	75.90	7.361	0.097	482	18.8	28,790	20.2	0.017345	0.27	347.57	0.92
20	KV-4	B	0.752	79.87	83.39	1.044	2,712	41.6	265,000	42.0	0.012732	0.34	255.72	0.86
21		B	0.792	94.28	111.5	1.183	4,116	36.0	323,000	36.4	0.015490	0.30	310.70	0.93
26	KV-5	B	1.754	91.19	3.528	0.039	454	44.6	29,640	47.6	0.018197	0.37	364.50	1.33
27		B	1.797	69.15	2.768	0.040	266	25.8	14,750	29.4	0.018277	0.37	366.08	1.36
32	KV-6	B	0.266	148.4	9.484	.064	511	144	50,760	150	0.018032	0.56	361.22	2.04
33		B	0.318	146.8	6.924	0.047	495	166	50,960	173	0.018627	0.63	373.02	2.35
34		B	0.851	145.0	19.54	0.135	2,423	154	259,700	155	0.018074	0.32	362.05	1.15
35		B	0.843	166.0	11.22	0.068	1,988	440	421,600	444	0.017405	0.36	348.77	1.26
72		Ap	6.725	3.226	93.43	28.96	209.5	0.21	9,120	0.32	0.018780	0.31	376.08	1.07
76	KV-8	Ap	6.578	2.781	62.43	22.45	160.4	0.21	6,501	0.33	0.018795	0.34	376.37	1.10
81	KV-18	Ap	4.854	3.375	151.8	44.96	224.5	0.20	9,893	0.40	0.018829	0.39	377.05	1.38
82		Ap	6.242	3.598	149.9	41.67	182.1	0.18	7,659	0.32	0.018785	0.34	376.18	1.15
45	115/85	Z	0.984	0.128	1124.0	8774	547,604	674	>1,000,000		0.018953	0.48	379.51	1.82
46		Z	0.866	0.089	648.9	7260	220,973	296	>1,000,000		0.018807	0.47	376.61	1.78
47		Z	0.709	0.103	668.1	6484	273,243	3060	>1,000,000		0.018775	0.42	375.96	1.59
49	127/85	Z	0.169	52.46	455.5	8.684	27,396	1108	>1,000,000		0.018897	0.41	378.39	1.55
50		Z	0.145	36.12	343.4	9.506	17,266	948	>1,000,000		0.018790	0.57	376.27	2.14
51		Z	0.392	34.64	275.8	7.963	27,054	256	>1,000,000		0.018901	0.32	378.47	1.21
52		Z	1.045	38.75	350.2	9.038	114,564	170	>1,000,000		0.018813	0.29	376.72	1.10
53		Z	0.576	52.75	418.7	7.938	63,883	1070	>1,000,000		0.018869	0.32	377.83	1.21
54	91500	Z	0.076	74.78	25.7	0.3439	2,011	116	88,960	116	0.053926	0.52	1061.60	5.52
55		Z	0.459	83.60	27.8	0.3321	7,726	191	480,200	191	0.054015	0.28	1063.30	2.97
59		Z 4)	0.177	78.97	26.8	0.3387	1,134	41.5	30,990	41.6	0.053827	0.43	1059.70	4.58
		Certified 5)		81.20	28.7	0.3443					0.053740	0.54	1057.80	5.50
62	61.308B	Z 4)	0.171	182.61	248.2	1.359	54.8	14.9	233,600	36.7	0.0001290	10.3	2.607	0.269
63		Z 4)	0.171	165.65	227.4	1.373	139	335	>1,000,000		0.0001265	5.92	2.558	0.151
		Certified 5)		218.00	409.4	1.710					0.0001264	1.00	2.554	0.026

1) Fraction numbers as in Tables 2 and 5.
2) Atomic ratios corrected for blank, spike, fractionation and initial common Pb. The 208Pb/204Pb ratios are corrected for spike fractionation, but not for procedure blank.
3) Ages are calculated relative to Pb isotopic composition in calcite from KV-5, the most primitive Pb analyzed in Kovdor, assuming that the calcite contains no Th.
4) Analyzed with 233U-236U-229Th-205Pb spike, all other analyses with 235U-230Th-205Pb spike.
5) Weighted average values with 95% confidence errors recalculated form Wiedenbeck et al. (1995) using ISOPLOT (Ludwig 1997).

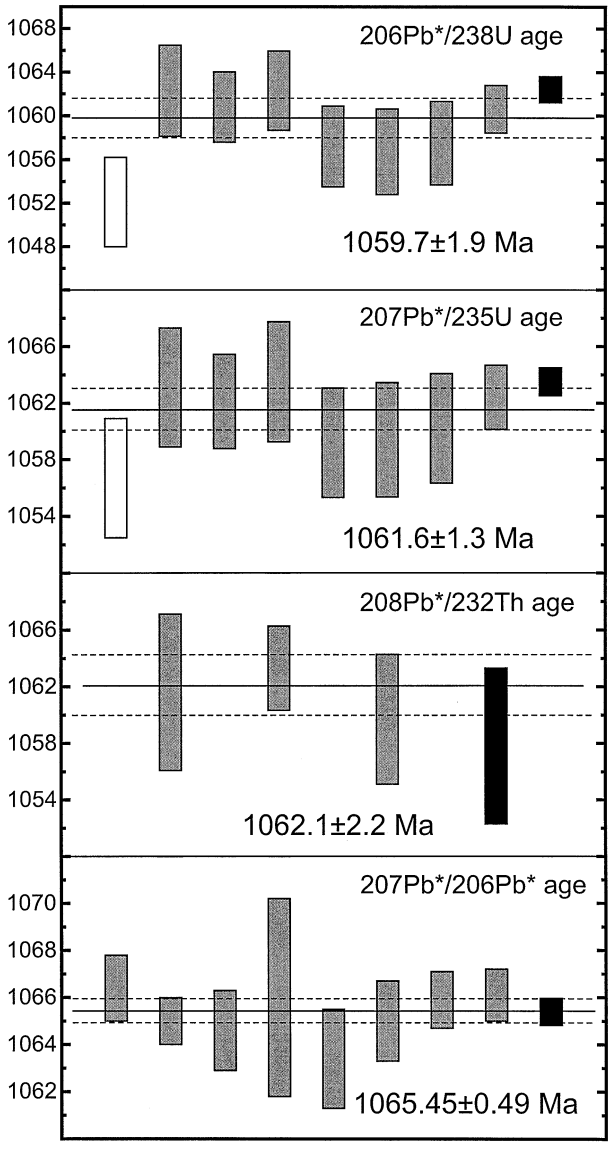

Fig. 3. Reproducibility of U-Th-Pb analyses of the standard zircon 91500. Data from Tables 2 and 3 (analyses 55 to 61 for $^{206}Pb/^{238}U$ and $^{207}Pb/^{235}U$, 54 to 59 for $^{208}Pb/^{232}Th$,a and 54 to 61 for $^{207}Pb/^{206}Pb$) are shown with grey 2σ error bars. U-Pb data for analysis 54, shown with open bars, are not included in the mean calculation (see text). Solid and dashed lines represent weighted means and 95% confidence intervals, respectively. The weighted means of measurements performed during the standard certification (recalculated from Wiedenbeck et al. (1995) using ISOPLOT, and plotted with 95% confidence errors) are shown for comparison with black bars.

Fractions of the very young standard zircon 61.308B (Wiedenbeck et al. 1995) were analysed for both U-Pb and Th-Pb, using the procedures described above. The results of three U-Pb analyses (Table 2) and two Th-Pb analyses (Table 3) are consistent with each other and with the results of Wiedenbeck et al. (1995), obtained on much larger fractions. From the combined data for the two standard zircons, and considering the calibration of the mixed spikes against multiple mixed normal solutions, we conclude that the U-Th-Pb data obtained in this study are likely to be accurate within quoted errors. Any statistically significant discrepancies in apparent ages between various mineral geochronometers and between different decay schemes are thus thought to be caused by the natural rather than analytical reasons, and are interpreted accordingly.

5.2. Standard Feldspar

The Rb-Sr data for the standard potassium feldspar SRM-607 are presented in Table 4. Four approximately 10 mg fractions of this powdered standard yielded slightly variable $^{87}Rb/^{86}Sr$ ratios, and $^{87}Sr/^{86}Sr$ ratios varying well outside of errors. The $^{87}Sr/^{86}Sr$ ratios are correlated with $^{87}Rb/^{86}Sr$, and we explain their variations to be a result of the sample heterogeneity. The model Rb-Sr ages, calculated relative to the initial $^{87}Sr/^{86}Sr$ value of 0.710 ± 0.001, are consistent within error and give a weighted average of 1410.4 ± 5.6 Ma (0.4%, 95% conf.), MSWD = 1.09. This model age is in close agreement with the value of 1409.0 ± 7.8 Ma, calculated from the NBS certified Rb and Sr concentrations, and with the values published by other authors, e.g., 1413.0 ± 4.4 Ma based on the data of Collerson et al. (1989). The two latter values are recalculated relative to the initial $^{87}Sr/^{86}Sr$ value of 0.710 ± 0.001.

5.3. Kovdor Baddeleyite

Baddeleyite is ubiquitous in the Kovdor carbonatites and phoscorites. In seven out of eight studied rocks baddeleyite forms relatively large (up to 2 to 3 mm) clear brown crystals. All the baddeleyite crystals found in the calcite carbonatite 1/84 are colourless. This unusual appearance suggested that this may be another mineral, but the XRD and microprobe analyses have confirmed mineral as baddeleyite. All samples except one contain visually homogeneous baddeleyite populations. The exception is the calcite carbonatite 244/76, which contains baddeleyite of various hues from pale-brown to black. Twinning of baddeleyite crystals is common in this sample, but is rarely seen in the other studied rocks.

Uranium concentration in baddeleyite (Table 2) varies from 20 to 190 ppm for the brown and colourless varieties. The black baddeleyite (fraction 7) has much higher U content of 909 ppm. Common Pb content is low in most fractions, but baddeleyite fractions from some samples (e.g., 1/84, KV-4 and KV-5) contain elevated common Pb amounts that correlate with the fraction size. This may result from the presence of microscopic inclusions of other minerals in baddeleyite crystals. We have studied several grains of baddeleyite from each sample using SEM and microprobe and have not detected inclusions of other minerals. However, epitaxic intergrowths of baddeleyite with pyrochlore or torianite are known in carbonatites (Evzikova 1960, Krasnova et al. 1967). Thorium concentration in baddeleyite (Table 3) varies greatly between samples. Baddeleyite fractions from three out of four studied phoscorites have Th contents of 1.6 to 19.5 ppm and Th/U ratios between 0.039 to 0.135, within the range of previously studied baddeleyite from various rocks (Heaman and LeCheminant 1993). The baddeleyite from the phoscorite KV-4 has unusually high Th content of $\sim$100 ppm and Th/U > 1.

All fractions of brown and colourless baddeleyite have $^{206}Pb/^{238}U$ ages between 373 to 380 Ma (Table 2 and Fig. 4a).

Table 4. Rb-Sr data.

Fraction number	Sample 1)	Fraction description	Fraction wt, mg	Rb ppm	Sr ppm	87Rb/86Sr	2 σ error 2)	87Sr/86Sr	2 σ error 3)	Model Age Ma 4)	2 σ error
		Kovdor Complex mica									
1	KV-5	1 rounded pale-green	0.111	236	25.96	26.63	0.27	0.84499	0.00012	373.1	4.0
2		1 pale-green irreg shape	0.462	213	41.27	15.04	0.16	0.78332	0.00004	372.7	4.6
3	KV-6	1 subhed bright green	0.761	234	45.74	14.92	0.18	0.78289	0.00002	373.6	5.0
4		1 subhed green zoned drk-light	0.304	218	16.64	38.58	0.40	0.90816	0.00006	372.6	3.9
5		1 rounded zoned green to yellow	0.373	203	39.65	14.95	0.16	0.78271	0.00003	372.2	4.5
6	KV-25	1 euhed zoned green-brown	0.191	306	10.88	84.81	0.87	1.15117	0.00019	370.8	3.8
7		1 euhed zoned green-brown	0.088	308	6.484	147.86	1.51	1.48428	0.00110	370.9	3.8
8	115/85	1 subhed blue	0.106	301	44.55	19.76	0.20	0.80831	0.00011	372.5	4.1
9		1 subhed zoned blue to orange	0.161	283	51.95	15.88	0.16	0.78786	0.00005	373.0	4.3
10		1 subhed orange	0.177	349	2.687	466.34	4.80	3.16338	0.00102	370.5	3.8
11		1 subhed orange	0.096	418	25.13	49.33	0.50	0.96661	0.00010	374.6	3.8
12	127/85	1 euhed orange-red	0.546	416	2.145	788.20	10.21	4.84600	0.00087	369.1	4.7
13		1 euhed orange-red	0.333	414	1.243	1926.92	22.12	10.9171	0.00862	372.3	4.2
14		1 euhed orange-red zoned drk-light	0.186	277	6.521	131.12	1.34	1.40399	0.00030	375.2	3.8
15		1 euhed orange-red zoned drk-light	0.183	238	0.783	1618.20	16.32	9.31900	0.01000	373.9	3.7
		Feldspar standard									
16	SRM-607		9.870	566	70.61	24.30	0.23	1.201252	0.000014	1409.7	13.2
17			9.230	572	71.74	24.19	0.30	1.202488	0.000013	1419.5	17.5
18			10.800	535	66.35	24.47	0.14	1.203421	0.000015	1405.6	8.5
19			12.500	522	65.60	24.14	0.19	1.200156	0.000013	1415.8	11.4

1) Rock names and intrusive phases are indicated in Table 1.
2) Errors in 87Rb/86Sr ratios are propagated to include most sources of uncertainty, most significant being Rb fractionation and within-run statistics.
3) Errors in 87Sr/86Sr are from within-run statistics.
4) Model ages are calculated relative to initial 87Sr/86Sr of 0.7035 ± 0.0005 for the Kovdor Complex micas, and 0.710 ± 0.001 for the feldspar standard, using decay constant of 87Rb of 1.42*10–11 y-1. Errors in model ages are propagated to include uncertainties in measured 87Rb/86Sr and 87Sr/86Sr, and initial 87Sr/86Sr. Error in 87Rb decay constant not included.

The black baddeleyite fraction has much younger $^{206}Pb/^{238}U$ age of 355 Ma. The analytical errors vary greatly with the relative content of common Pb. To minimise the effect of uncertainty in the common Pb correction on precision and accuracy of the ages, we shall only consider baddeleyite analyses with $^{206}Pb/^{204}Pb > 3000$, which comprise 82% of the total number of analyses. These high-precision data, shown in Figure 4b, form a compact cluster with the $^{206}Pb/^{238}U$ age of ca. 378 Ma and the $^{207}Pb/^{235}U$ age of ca. 381 Ma. All the analyses show normal discordance of 3 to 6%, well outside of the error limits. The nature of this discordance is not obvious, and therefore no precise and accurate age information can be derived from these data without detailed consideration. Here we only note that the analytical points with the same values but larger random errors would appear concordant. It is clear that an attempt to artificially exaggerate the errors to make the data points seem concordant is the way of hiding the problem rather than solving it, which would add an uncontrolled systematic error to the calculated age.

The $^{208}Pb/^{232}Th$ ages of the baddeleyite fractions vary widely between 255 Ma and 425 Ma (Table 3). Excluding the fraction 14 with the lowest $^{208}Pb/^{204}Pb = 84$ reduces the range to 255 to 373 Ma. This range of variations is 17 times larger than the range of $^{206}Pb/^{238}U$ ages of the same fractions. Moreover, all baddeleyite $^{208}Pb/^{232}Th$ ages are younger than the $^{206}Pb/^{238}U$ ages, and the scatter of the $^{208}Pb/^{232}Th$ ages does not correlate with $^{208}Pb/^{204}Pb$ ratios (the measure of radiogenic lead to common lead ratio for the Th-Pb system). This suggests that the variations in the $^{208}Pb/^{232}Th$ ages could have been caused by preferential loss of radiogenic ^{208}Pb, rather than by uncertainty in the common Pb correction.

5.4. Kovdor Zircon

Abundant zircon was recovered from the carbonatites 127/85 and 115/85. In the dolomite carbonatite 115/85 zircon is a rock-forming mineral, which makes up ~20 to 30% of the rock volume. Large zircon crystals (>5 mm) were broken into fragments, and some fragments were abraded before analysis. A peculiar feature of zircon from the calcite carbonatite 127/85 is the presence of numerous very thin and long, fibre-shaped inclusions. Semiquantitative SEM-EDS data suggest that this mineral belongs to the amphibole group. We have analysed fractions rich with these inclusions, as well as fractions free of visible imperfections.

Crystal cell dimensions of zircon from the carbonatite 115/85 were determined at the ROM using X-ray diffraction to yield a = 6.617 Å, c = 5.989 Å. These values are similar to those of the standard zircon G42778 (Wiedenbeck et al. 1995) analysed for comparison: a = 6.613 Å, c = 5.998 Å, and are

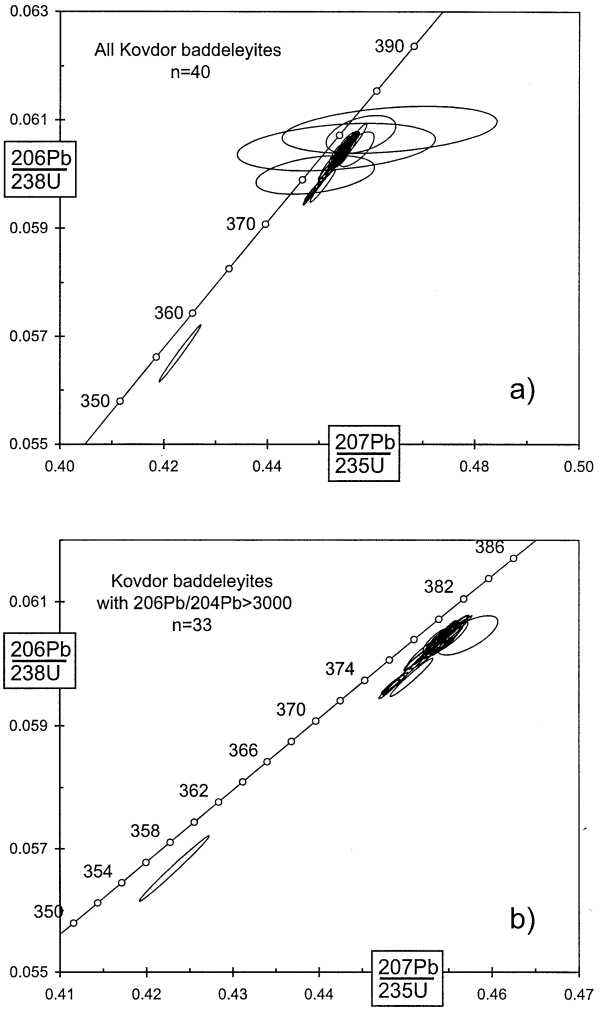

Fig. 4. Concordia diagrams showing baddeleyite U-Pb data. a) All data; b) Fractions with $^{206}Pb/^{204}Pb > 3000$. The fraction with low $^{206}Pb/^{238}U$ age of 355.4 Ma is a high-U black baddeleyite from sample 244/76 (fraction 7).

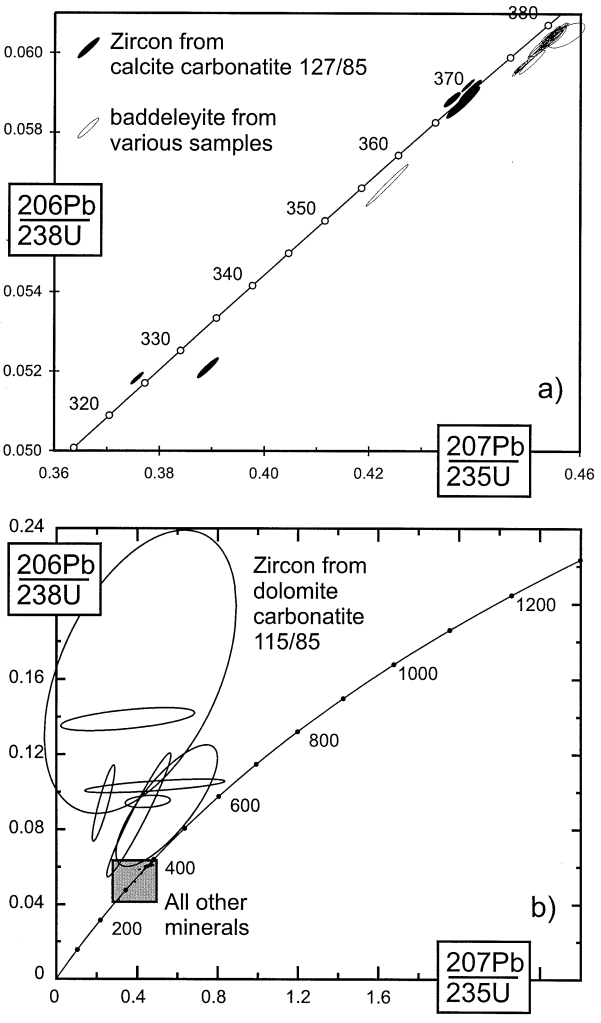

Fig. 5. Concordia diagrams showing zircon U-Pb data. a) Zircon with uranium content of 34 to 52 ppm and Th content of 275 to 455 ppm from the calcite carbonatite 127/85 (filled ellipses). Baddeleyite data are shown for comparison. b) Zircon with uranium content of 0.06 to 0.21 ppm and Th content of 648 to 1124 ppm from the dolomite carbonatite 115/85. Grey square on concordia line covers the range of all other zircon, baddeleyite and apatite data. The comparison between these data shows that 50 to 80% of all radiogenic ^{206}Pb in the dolomite carconatite zircons are generated by decay of initial excess ^{230}Th.

within the range of the published values for a crystalline zircon with undamaged structure (e.g., Holland and Gottfried 1955).

Zircon from the calcite carbonatite 127/85 has a relatively low U content of 29 to 53 ppm, elevated Th content of 275 to 455, and Th/U ratios of 7.9 to 9.5. The U-Pb data are shown in a concordia diagram in Figure 5a. Four out of six fractions cluster near concordia at 367 to 369 Ma, while the other two fractions show much lower ages close to 330 Ma. Three out of six fractions show reverse discordance, presumably as a result of the presence of unsupported ^{206}Pb, formed by decay of initial excess ^{230}Th (Mattinson 1973, Ludwig 1977, Schärer 1984).

Zircon from the dolomite carbonatite 115/85 has extremely low uranium content of 0.06 to 0.21 ppm, very high Th content of 650 to 1120 ppm, and Th/U ratios of 6484 to 8774. These are probably the highest values of Th/U ratios determined in a zircon so far. U-Pb age determinations are not possible for these zircons (Fig. 5b) because the radiogenic ^{206}Pb content is dominated by unsupported Pb, whereas the content of radiogenic ^{207}Pb is too small to be measured and corrected for common Pb with sufficient precision.

In contrast to the U-Pb system, the ^{208}Pb-^{232}Th system in both carbonatite zircons (Table 3) yielded consistent ages. The weighted average ^{208}Pb-^{232}Th age of all five analysed zircon fractions from the calcite carbonatite 127/85 is 377.6 ± 1.1 Ma (MSWD=1.8). The three fractions from the dolomite carbonatite 115/85 yield the weighted average ^{208}Pb-^{232}Th age of 377.2 ± 4.6 Ma (MSWD = 4.6). All these eight fractions from both samples calculated together give the age of 377.52 ± 0.94 Ma (MSWD = 2.4).

5.5. Kovdor Apatite and Calcite

Both apatite and calcite are common primary minerals in phoscorites and carbonatites. Apatite was analysed from six

phoscorites of various phases, and from three carbonatites. Uranium and thorium contents of 0.2 to 3.6 ppm, and 62 to 150 ppm, respectively (Tables 3 and 5) suggest that apatite may yield precise U-Pb and Th-Pb ages, if precise and accurate initial Pb isotopic composition can be determined. The coexisting and presumably cogenetic calcite appeared to have low U content (<1 ppb to 90 ppb, Table 5). The $^{238}U/^{204}Pb < 1$ in five out of seven analysed fractions results in very small or negligible radiogenic Pb growth over the period of ca. 380 Ma, therefore the Pb isotopic compositions measured in low-U calcite can represent the Pb isotopic composition in the magma.

Several approaches can be used to calculate U-Pb and Th-Pb ages of minerals containing comparable amounts of radiogenic and common Pb: $^{238}U/^{204}Pb$-$^{206}Pb/^{204}Pb$, $^{235}U/^{204}Pb$-$^{207}Pb/^{204}Pb$, $^{232}Th/^{204}Pb$-$^{208}Pb/^{204}Pb$ and $^{207}Pb/^{204}Pb$-$^{206}Pb/^{204}Pb$ isochrons, and calculating radiogenic $^{206}Pb^*/^{238}U$ and $^{207}Pb^*/^{235}U$ ages assuming certain initial Pb. In addition, the three-dimensional linear total Pb/U isochron has been proposed (Ludwig 1998) for calculating ages of series of cogenetic samples with an undisturbed U-Pb system that shares the same common-Pb isotopic composition, but has variable ratio of radiogenic Pb to common Pb. The total Pb/U isochron uses all of the relevant isotope ratios at the same time, yielding the smallest justifiable age-error of any possible U/Pb or Pb/Pb isochron (Ludwig 1998). If the initial Pb composition in the Kovdor massif is uniform, the total Pb/U isochron would be a preferred method of age calculation for the apatite and calcite. Application of this method to all analysed apatites and calcites (Fig. 6) yields the age of 380.6 ± 2.6 Ma (MSWD = 38), and initial $^{206}Pb/^{204}Pb = 18.724 \pm 0.042$, $^{207}Pb/^{204}Pb = 15.528 \pm 0.048$. The conventional $^{238}U/^{204}Pb$-$^{206}Pb/^{204}Pb$ and $^{235}U/^{204}Pb$-$^{207}Pb/^{204}Pb$ isochrons for the same analyses yield 380.6 ± 3.4 Ma (MSWD = 87.2) and 379.0 ± 9.3 Ma (MSWD = 5.4), consistent with the total Pb/U isochron age.

Regressions of apatite analyses only yielded the total Pb/U isochron age of 377.5 ± 3.5 Ma (MSWD = 27), the $^{238}U/^{204}Pb$-$^{206}Pb/^{204}Pb$ isochron age of 377.5 ± 6.1 Ma (MSWD = 42), and the $^{235}U/^{204}Pb$-$^{207}Pb/^{204}Pb$ isochron age of 366 ± 19 Ma (MSWD = 5.8). These apparent ages are within error of the combined apatite + calcite values, but are less precise because of a smaller range of U/Pb ratios.

Variations in the measured and initial (at 380 Ma) $^{206}Pb/^{204}Pb$ ratios of the five low-U calcites indicate initial Pb isotope heterogeneity between igneous phases. Pooling together the data from different samples on the same isochron may be thus not strictly correct, and the weighted means of individual $^{206}Pb^*/^{238}U$ and $^{207}Pb^*/^{235}U$ ages calculated using the calcite Pb from the same sample may be more accurate. We have not analysed calcite from the phoscorite KV-2, but used the most primitive measured calcite Pb for common Pb correction. The data from this sample are therefore not included in the mean age calculations. The weighted mean of individual $^{206}Pb^*/^{238}U$ ages of apatites with [U] > 1 ppm, corrected using $^{206}Pb/^{204}Pb$ in the coexisting calcite (data from Table 5), is 379.9 ± 1.7 Ma, MSWD = 16. The weighted mean of $^{207}Pb^*/^{235}U$ ages calculated using the same approach is 378.5 ± 6.9 Ma, MSWD = 2.3. These results are well within error of the pooled isochron ages.

Four out of five apatite fractions (all except KV-2) analysed for Th-Pb yield the weighted mean of $^{208}Pb^*/^{232}Th$ ages of 376.4 ± 0.6 Ma, MSWD = 0.46. This age is slightly younger than the mean $^{206}Pb^*/^{238}U$ age of the same apatite fractions, and is within error of the mean $^{208}Pb^*/^{232}Th$ age of the carbonatite zircons.

5.6. Kovdor Mica

We have analysed fifteen single grains of phlogopite and tetraferriphlogopite from two phoscorites and three carbonatites. Choosing mica grains of varying appearance (Table 4) yielded broad spread of Rb/Sr ratios from 15 to 1600, and allowed us to obtain precise isochron Rb-Sr age. Individual isochron ages for all five samples are between 371.1 ± 10.1 Ma and 373.7 ± 9.9 Ma, and all agree within errors. Initial $^{87}Sr/^{86}Sr$ ratios calculated from these isochrons, between 0.703 ± 0.015 and 0.7099 ± 0.0092, are also consistent within error. A regression through all fifteen data points (Fig. 7) yielded the age of 372.2 ± 1.5 Ma and the initial $^{87}Sr/^{86}Sr = 0.70368 \pm 0.00055$ (MSWD = 0.67).

6. DISCUSSION

On the whole, the ages obtained from various isotopic systems in various minerals indicate that the Kovdor carbonatites and phoscorites are ~372 to 380 m.y. old. In detail, however, the age pattern is very complex, and the apparent ages disagree well outside of the error limits. To obtain the precise and reliable age of the massif and its constituent phases, we need, first of all, to evaluate all possible factors that may influence the accuracy of various geochronometers.

6.1. U-Pb and Th-Pb Systems in Apatite and Zircon

None of the studied minerals (zircon, baddeleyite, apatite), and none of the three decay schemes (^{238}U-^{206}Pb, ^{235}U-^{207}Pb, ^{232}Th-^{208}Pb) can be a priori assumed to be free of distortion. Zircon has consistent ^{232}Th-^{208}Pb but erratic U-Pb systematics. Baddeleyite shows discordance between the ^{238}U-^{206}Pb and ^{235}U-^{207}Pb systems, and, in addition, irregular variations in ^{232}Th-^{208}Pb ages. Apatite contains relatively large amounts of common Pb, and its U-Th-Pb ages are thus sensitive to the common Pb correction.

The age discrepancies might have been caused by a number of reasons. Two potential sources of inaccuracy are obvious: erroneous common Pb correction for apatite, and initial excess ^{230}Th in zircon and possibly in apatite. Other potential problems including variations in closure temperature between minerals, migration of radiogenic Pb, initial excess of ^{231}Pa, and inaccurate decay constants may be suspected but are more difficult to verify. The uncertainty in common Pb correction for apatite appears to be the least dangerous of these geochronological pitfalls. Several lines of evidence show that, despite relatively large common Pb correction and the scatter of points in isochron diagrams, the apatites yield accurate ages. All three decay schemes (^{238}U-^{206}Pb, ^{235}U-^{207}Pb and ^{232}Th-^{208}Pb) yielded compatible ages, regardless of widely varying fraction of radiogenic Pb in the total Pb: 0.6 to 6% for ^{207}Pb, 15 to 50% for ^{206}Pb, and 70 to 80% for ^{208}Pb. The ages calculated from the apatite data alone, and from the apatite and calcite data together, also agree within error. The agreement between the pooled isochron results, and the weighted means of apatite-

Table 5. Apatite and calcite U-Pb data.

						Atomic ratios 3)								Apparent ages, Ma 4)				Initial Pb ratios at 378 Ma 5)			
No 1)	Sample	Fraction	Fraction wt, mg	U ppm	Pb pmm 2)	238U/ 204Pb	2σ err	206Pb/ 204Pb	2σ err	207Pb/ 204Pb	2σ err	208Pb/ 204Pb	2σ err	206Pb/ 238U	2σ err	207Pb/ 235Pb	2σ err	206Pb/ 204Pb (T)	2σ err	207Pb/ 204Pb (T)	2σ err
65	KV-2	Ap	34.060	2.62	1.78	237.98	0.83	33.036	0.046	16.277	0.026	136.866	0.296	378.3	1.3	377.8	13.8				
66		Ap	9.027	2.49	1.82	223.78	0.51	32.544	0.030	16.294	0.018	139.690	0.232	388.2	1.0	404.8	12.2				
67	KV-5	Ap	29.730	2.04	1.49	274.12	0.60	35.350	0.042	16.427	0.022	143.579	0.304	381.2	1.0	389.0	10.9				
68		Cc	12.766	0.0002	1.62	0.0091	0.0001	18.654	0.022	15.499	0.024	38.351	0.074					18.653	0.022	15.499	0.024
69	KV-6	Ap	21.530	1.19	0.89	304.55	1.49	37.229	0.092	16.516	0.024	207.894	0.872	378.4	1.8	372.2	10.8				
70		Cc	10.960	0.0121	1.28	0.6045	0.0021	18.855	0.024	15.540	0.026	38.838	0.078					18.818	0.024	15.538	0.026
71		Ap	5.080	0.719	1.01	79.462	0.73	23.875	0.084	15.878	0.052	88.038	0.520	397.8	5.8	471.5	6.2				
72		Ap	6.725	3.23	2.42	304.73	0.80	37.338	0.050	16.554	0.023	209.630	0.440	380.3	0.9	384.1	10.5				
73		Ap	10.587	3.18	2.45	292.58	0.64	36.630	0.039	16.514	0.021	205.840	0.370	381.0	0.9	384.2	10.6				
74	KV-8	Cc	13.330	0.064	1.55	2.6397	0.016	18.888	0.016	15.545	0.018	38.660	0.058								
75		Ap	5.400	2.36	1.79	217.40	1.01	31.969	0.066	16.240	0.036	141.551	0.350	381.2	1.8	374.6	17.3				
76		Ap	6.578	2.78	1.84	280.26	0.88	35.877	0.051	16.469	0.024	160.540	0.340	382.9	1.1	383.5	9.9				
77	KV-9	Ap	26.970	0.52	1.02	41.371	0.18	21.405	0.028	15.691	0.026	55.010	0.100	397.4	4.5	481.5	69.8				
78		Cc	5.256	0.0004	1.85	0.0143	0.0004	18.775	0.020	15.509	0.022	38.438	0.070					18.744	0.020	15.509	0.022
70	KV-18	Cc	22.368	0.0071	2.80	0.1614	0.0013	18.679	0.028	15.531	0.028	38.784	0.082					18.669	0.028	15.530	0.028
80		Ap	24.800	3.19	3.40	233.55	1.19	32.754	0.052	16.254	0.028	238.065	0.558	377.5	1.8	361.1	15.9				
81		Ap	4.854	3.38	3.75	212.95	0.84	31.576	0.039	16.225	0.022	224.630	0.449	379.3	1.6	377.1	15.7				
82		Ap	6.242	3.60	4.01	177.88	0.42	29.431	0.036	16.104	0.023	182.230	0.336	378.7	1.4	373.5	19.1				
83	KV-21	Cc	3.350	0.088	1.68	3.3981	0.021	19.163	0.038	15.598	0.032	39.219	0.092								
84		Ap	7.560	0.214	0.70	24.422	0.076	20.345	0.030	15.657	0.026	55.526	0.108	352.5	13.3	332.0	194.0				
85	KV-25	Cc	10.270	0.031	2.25	0.8915	0.0032	18.677	0.014	15.533	0.016	38.969	0.056					18.622	0.014	15.530	0.016
86		Ap	9.230	2.11	1.64	154.72	0.41	27.883	0.026	16.003	0.020	93.971	0.146	374.7	1.1	357.0	15.8				

1) Fraction numbering continues from Table 2.
2) Total Pb content corrected for spike and fractionation, but not for procedure blank.
3) Atomic ratios corrected for blank, spike, fractionation and initial common Pb.
4) Ages calculated from slopes of two-point 206Pb/204Pb vs 238U/204Pb and 207Pb/204Pb vs. 235U/204Pb isochrons for apatite and coexisting calcite. Ages of apatites from sample KV-2 are calculated relative to calcite from KV-5, having the most primitive Pb isotopic compositions among all analyzed calcites.
5) Only initial Pb isotopic ratios for calcite fractions with measured 238U/204Pb <1 are included.

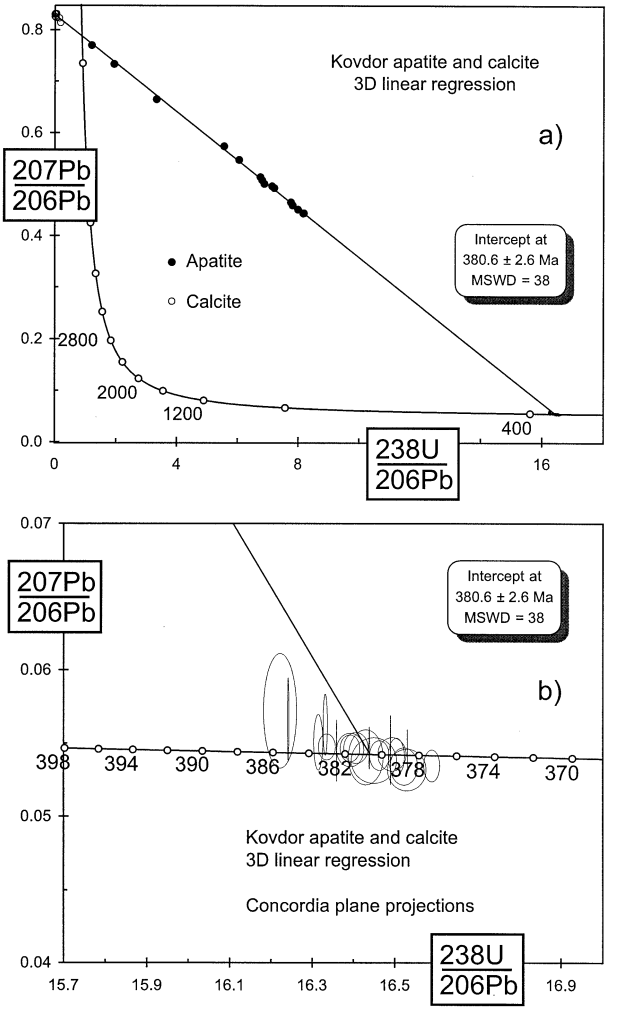

Fig. 6. U-Pb apatite and calcite data and total Pb-U 3-D linear regression. $^{207}Pb/^{206}Pb$ and $^{238}U/^{206}Pb$ ratios are not corrected for initial common Pb. a) Data plotted in the Tera-Wasserburg concordia diagram; b) Concordia plane projections.

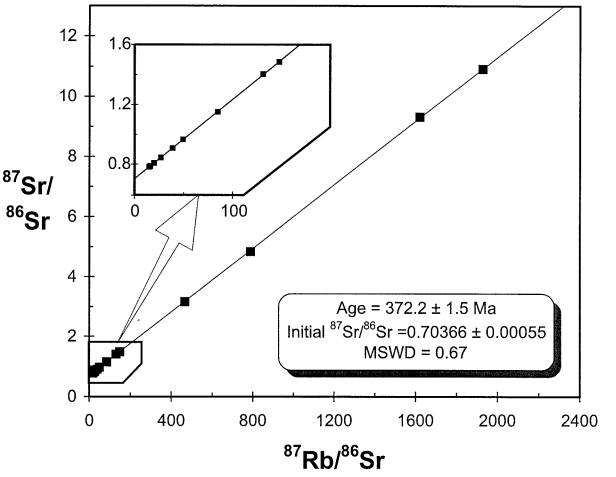

Fig. 7. Rb-Sr isochron diagram for single grain phlogopite and tetraferriphlogopite analyses from the Kovdor phoscorites KV-5 and KV-6, and carbonatites KV-25, 115/85, and 127/85. Error bars are smaller than the plotting symbols.

calcite ages of individual samples, indicates that the influence of the initial Pb isotopic variations on the apatite U-Th-Pb ages is insignificant. Elevated Th/U ratios of 22 to 45 suggest the likely presence of unsupported ^{206}Pb from the decay of initial excess ^{230}Th. The ^{206}Pb-^{238}U ages of apatites + calcites, whether the pooled isochron or the weighted mean of individual sample ages, are older than the ^{207}Pb-^{235}U ages by ca. 1.5 Ma. Taken at the face value, this difference is consistent with the first-order assumption of the apatite growth from a magma with Th/U between 2 and 4, with uranium-series isotopes in the magma in secular equilibrium. The difference between the ^{206}Pb-^{238}U and ^{207}Pb-^{235}U ages is, however, well within the error limits.

The U-Th-Pb data thus constrain the age of the Kovdor apatites at 380 to 376 Ma. There are good reasons to believe that this is the age of the apatite growth from the magma, rather than the timing of cooling. The diffusion of Pb in apatite (Watson et al. 1985, Cherniak et al. 1991) is slow enough so that the closure temperature of the U-Th-Pb system in the Kovdor apatite, mostly large equant crystals with all dimensions >1 mm, would be >600°C at a cooling rate >10°C/Ma, typical for cooling of an intrusive body emplaced in a relatively cold crust. This estimate is similar to the closure temperature of 620°C, obtained by Krogstad and Walker (1994) for large apatites from the slowly cooled Tin Mountain pegmatite. The estimated closure temperature is close to the homogenisation temperature range of 620 to 870°C for melt inclusions in the Kovdor apatite (Veksler et al. 1998a), suggesting that the apatites were closed for U, Th and Pb diffusion shortly after their crystallisation.

The Th-Pb age of 377.5 Ma of zircon, a mineral with still slower diffusion of U, Th and Pb (Cherniak et al. 1997, Lee et al. 1997, Cherniak and Watson 2000), further supports the crystallisation of the Kovdor carbonatites at 380 to 376 Ma. The ^{232}Th decay chain contains no long-lived intermediate products, so the $^{232}Th/^{208}Pb$ ages of both apatite and zircon are not notably affected by initial disequilibrium. We can therefore suspect that the apparent ages of other Kovdor minerals that are outside of the 380 to 376 Ma interval, have been biased by the problems like open geochemical systems, initial disequilibrium in U decay chains, or inaccurate decay constants.

6.2. U-Pb Age of Baddeleyite and Significance of Pb Loss

With the age frame of 380 to 376 Ma for the Kovdor phoscorite and carbonatite crystallisation established by the U-Th-Pb apatite and Th-Pb zircon data, we can evaluate the significance of the baddeleyite U-Pb data. The baddeleyite $^{207}Pb/^{235}U$ ages of 380 to 382 Ma, and in particular the $^{207}Pb/^{206}Pb$ ages of 390 to >400 Ma (Fig. 8a) outside of the 380 to 376 Ma limits. The anomalously old $^{207}Pb/^{206}Pb$ ages cannot be explained by Pb or U loss, and the discrepancy is too large to be related to inaccurate decay constant of ^{235}U (Ludwig 2000, Mattinson 2000). This may suggest the presence of excess ^{207}Pb. We can therefore rely only on the $^{206}Pb/^{238}U$ chronometer for a precise and accurate age determination of the baddeleyites. The variations in the $^{206}Pb/^{238}U$ baddeleyite ages, plotted in a histogram in Figure 8, however indicate the loss of

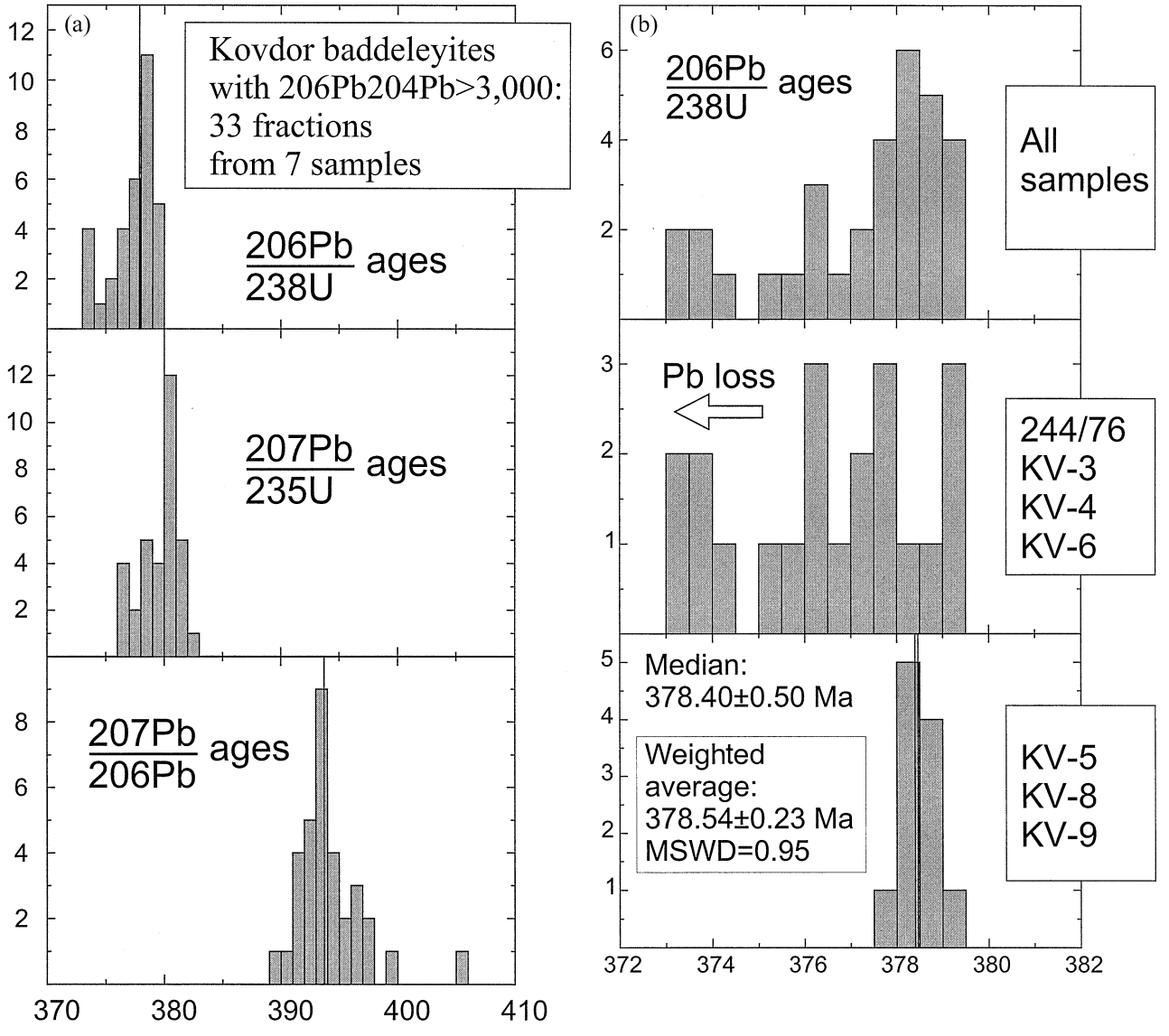

Fig. 8. Histograms of U-Pb and Pb-Pb ages of the Kovdor baddeleyites. All data with 206Pb/204Pb are included. a) comparison between $^{206}Pb/^{238}U$, $^{207}Pb/^{235}U$ and $^{207}Pb/^{206}Pb$ ages. b) Comparison between $^{206}Pb/^{238}U$ baddeleyite ages of two groups of samples—those that suffered minor Pb loss (244/76, KV-3, KV-4, KV-6), and samples with uniform $^{206}Pb/^{238}U$ ages and no detectable Pb loss (KV-5, KV-8, KV-9). More detailed explanation is in the text.

1 to 2% of radiogenic Pb from many of the analysed baddeleyites. A variable Pb loss of up to a few percent is common in baddeleyite (e.g., Heaman et al. 1993, Amelin et al. 1999). The high-U black baddeleyite from the phoscorite 244/76 has low $^{206}Pb/^{238}U$ age, possibly as a result of the Pb loss related to radiation damage (the U content and therefore the dose is 5 to 40 times higher for this fractions than for all other analysed baddeleyites).

An interesting feature of the $^{206}Pb/^{238}U$ data for the Kovdor baddeleyite is that some of the samples show ~10 m.y. age variations between fractions, while the others yielded consistent ages (Fig. 8 b). If the Pb loss is a recent subsurface process, then this difference may be related to the variations in the rock fracturing and in the paths of ground water migration, which result in a variable degree of weathering. Baddeleyite fractions from the phoscorites KV5, KV-6 and KV-9 have $^{206}Pb/^{238}U$ ages that agree within error, and probably were not affected by weathering and Pb loss. All eleven fractions from these samples yielded the weighted mean $^{206}Pb/^{238}U$ age of 378.54 ± 0.23 Ma, MSWD = 0.95. The quoted uncertainty includes all sources of random errors known to us, but does not include possible systematic errors in the decay constant of ^{238}U, and in the composition of normal solutions. This age is close to the upper limit of all baddeleyite $^{206}Pb/^{238}U$ ages, and this observation further supports the absence of Pb loss in baddeleyite from the phoscorites KV5, KV-6 and KV-9.

There is strong evidence that the age of 378.54 ± 0.23 Ma is accurate. All these baddeleyite fractions have $^{206}Pb/^{204}Pb$ ratios >7000, and the uncertainty in common Pb correction is negligible. Very low Th/U ratios suggest the initial deficiency

in ^{230}Th, but, unlike the initial excesses, it is easy to quantify. Correction of the initial ^{230}Th deficiency for Th/U$<<$1 in baddeleyite gives the age 378.64 Ma. We consider this age as the most precise estimate for the timing of crystallisation of the Kovdor phoscorites.

6.3. Evidence for Differential Mobility of Uranogenic and Thorogenic Pb

There is a marked contrast between Th-Pb and U-Pb patterns in zircon from the carbonatite 127/85. All five fractions analysed for ^{232}Th/^{208}Pb yielded invariable ages, which are also consistent with the best baddeleyite ^{206}Pb/^{238}U age, and with the apatite Th-U-Pb ages. This is strong evidence for closed ^{232}Th/^{208}Pb system in the zircon. On the contrary, the U-Pb ages of the same fractions (Fig. 5a) are younger and widely variable, providing clear evidence for Pb loss. These results are not dependent on initial Pb correction, since all the fractions have very radiogenic Pb with ^{206}Pb/^{204}Pb $>$ 5000. Small variations in ^{206}Pb/^{238}U might certainly result from excess ^{230}Th, but the large correlated variations can hardly be explained by any mechanism other than recent Pb loss.

The pattern shown by the baddeleyite is the opposite. The ^{206}Pb/^{238}U ages of the baddeleyite are reasonably consistent, and, with the exception of the high-U fraction, show only a small range of age variations about two percent. In contrast, the variations in the apparent ^{208}Pb/^{232}Th ages are 17 times as large, and all ^{208}Pb/^{232}Th ages are younger than the ^{206}Pb/^{238}U ages. Again, this pattern cannot be explained by an uncertainty in common Pb correction (^{208}Pb/^{204}Pb ratios are from 260 to $>$4000, much higher than in the apatites), or by initial isotopic disequilibrium, but agrees with the higher mobility of radiogenic ^{208}Pb as compared to ^{206}Pb in baddeleyite.

The difference in mobility of uranogenic and thorogenic Pb has been previously reported for zircon (Steiger and Wasserburg 1966) and allanite (Barth et al. 1994). The notable feature of all these examples of differential Pb mobility is that the isotopic system that includes more abundant parent element (U in our baddeleyite, and in zircon of Steiger and Wasserburg, 1966, and Th in our zircon and in allanite of Barth et al., 1994), is more stable. If the differential mobility of radiogenic Pb was caused by radiation damage, then radiogenic Pb produced from the more abundant radioactive parent would be more mobile, opposite to our observations. Another important feature is that Th/U ratios in all these minerals are strongly fractionated relative to their abundances in the source. All these observations can be explained by the difference in structural position of U and Th in the crystal lattice: the more abundant element replaces a main component (e.g., U replaces Zr in baddeleyite), while the less abundant one (e.g., Th in baddeleyite) is effectively excluded from the lattice during crystal growth, and is located in crystal imperfections: dislocations, micro-fractures, alteration zones, and/or in microscopic inclusions of a different mineral phase. Checking this possibility would require a detailed mineralogical study of minerals with high and low Th/U ratios.

If our explanation of differential Pb mobility is correct, it may be expected that baddeleyite from various rocks would have better preserved U-Pb than Th-Pb, and Th-Pb system in monazite would be typically more stable than U-Pb, whereas in the minerals with more variable chemical compositions (apatite, perovskite), which can easily accommodate both U and Th, the stability of both U-Pb and Th-Pb systems is likely to be similar. Our explanation for differential mobility of radiogenic Pb can be further checked against the results of other comparative U-Pb and Th-Pb geochronological studies. Unfortunately these studies are sparse, because in the modern geochronological practice the Th-Pb system is commonly considered redundant and is rarely used to complement the U-Pb dating.

6.4. Extreme Elemental Fractionation and Initial Disequilibrium in the Uranium Decay Chains

Two out of three minerals, analysed for U-Th-Pb in this study, zircon and apatite, have Th/U ratios from 20 to almost 10000. These values are much higher than in any common mantle and crustal rocks, and indicate a high degree of chemical fractionation of Th from U during magma evolution and mineral growth. This fractionation resulted in the enrichment in ^{230}Th relative to its long-lived parent nuclide ^{238}U (Mattinson 1973, Ludwig 1977, Schärer 1984, Barth et al. 1989). If the initial abundance of ^{230}Th, ^{231}Pa and other intermediate U-series nuclides in the studied mineral is known, then the excess or deficiency in radiogenic ^{206}Pb and ^{207}Pb can be calculated and used to correct ^{206}Pb/^{238}U and ^{207}Pb/^{235}U ages. The abundance of ^{230}Th in a growing mineral can be estimated from Th/U ratios in the mineral and the parental magma, and the known degree of disequilibrium in the magma.

This approach was used by Schärer (1984) and in some subsequent studies (e.g., Parrish 1990) to correct ^{206}Pb/^{238}U in monazites for unsupported ^{206}Pb, produced by decay of initial excess ^{230}Th. Two simplifying assumptions were taken: the parental magma is assumed to be in secular equilibrium, and the Th/U ratio in melt is approximated by the Th/U ratio in the host rock. The correction was found to improve concordance of the data, however we think that in general the above assumptions are unverifiable, and may be invalid in many cases.

Both of these assumptions are probably inapplicable to carbonatites and related rocks. The U-series studies of the lavas from the modern carbonatite volcano Oldoinyo Lengai (Williams et al. 1986, Pyle et al. 1991) show high degrees of disequilibrium between U, Th and Ra isotopes, probably the most extreme among all studied modern volcanics. This disequilibrium may be caused by chemical fractionation during magma generation, and separation of immiscible carbonate and silicate liquids, as shown by experimental data of Jones et al. (1995) and Veksler et al. (1998b). In addition, early crystal fractionation of a mineral strongly enriched in U or Th (e.g., baddeleyite, perovskite) would leave uranium-series nuclides in the residual melt in disequilibrium. All of these mechanisms of fractionation are common in carbonatite genesis, so it is likely that U-series nuclides on parental magmas of intrusive carbonatites were far from secular equilibrium.

Using Th/U in the host rock is as a proxy for the Th/U ratio in the magma is not necessarily a valid assumption either. The composition of the host rock of the studied minerals by no means can serve as a chemical proxy for the parent medium from which these minerals grew. Using the host rock as a chemical proxy for the parent magma may be reasonable for accessory mineral phenocrysts in volcanic rocks (e.g., zircon in

a rhyolite). However, it is a poor assumption for cumulate igneous rocks, due to crystal precipitation and evolution of the melt during crystallization. The host rock in this case is a combination of various cumulate minerals and crystallised intercumulus liquid, rather than the parent melt. Moreover, equating parent magma with host rock is basically wrong and can produce misleading results if applied to pegmatites or any other rocks that precipitate from a flow of a fluid or volatile-rich melt. In the latter case the medium from which the minerals grew may only be found in the fluid/melt inclusions. The composition of the parent melt of the coarse-grained zircon-rich carbonatites is unknown, but it must have been very different from their bulk rock composition. Because neither the Th/U ratio not the equilibrium/disequilibrium state of the parental melts of high-Th/U Kovdor apatite and zircon are known, we cannot make any justifiable corrections for excess ^{230}Th. But the high Th/U ratios and combined U-Th-Pb isotopic systematics provide reliable qualitative evidence for the presence of large initial excess of ^{230}Th.

In the decay chain of ^{235}U, the only relatively long-lived intermediate nuclide is ^{231}Pa. Unlike thorium, protactinium has no stable or long-lived extant isotopes, therefore any speculations about the ^{231}Pa disequilibrium have to rely on using another element as a geochemical proxy. This makes even qualitative estimates more uncertain than for the ^{230}Th-^{238}U systematics. In aqueous systems both Th and Pa are essentially insoluble and are scavenged by particles, although at slightly different rates (e.g., Walter et al. 1997). The difference in the Th and Pa behaviour is, however, very small compared to the difference between these elements and U, so Th can serve as a first-order proxy for Pa. In contrast, the behaviour of Pa in magmatic systems is poorly known and may be very different from that of ^{232}Th. We are not aware of any experimental data on Pa partitioning between carbonate or silicate melts and crystallising solids, and therefore have to rely on speculations based on valence and ionic radii. Since the oxygen fugacity of carbonatite-phoscorite melts is sufficiently high $1\tilde{0}^{-19}$ to 10^{-17} bar (Friel and Ulmer, 1974, Treiman and Essene, 1984), then protactinium exists predominantly in Pa^{5+} state (e.g., Barth et al. 1989). In this case Pa can be expected to behave similarly to Nb^{5+} and Ta^{5+}, rather than to much larger tetravalent Th and U. Baddeleyite from the Kovdor carbonatites and phoscorites is very rich in Ta and Nb (up to 6700 ppm and 17500 ppm respectively, Williams 1996, Williams and Zaitsev, unpubl. data), and has extremely fractionated Nb/Ta ratios between 1 and 4, ~5 to 15 times lower than the bulk earth value. This supports the possibility of high enrichment in Pa relative to U in baddeleyite.

Large excesses of ^{207}Pb were described by Mortensen et al. (1992, 1997) in pegmatite zircons, and the excess ^{231}Pa was proposed as a likely source of unsupported ^{207}Pb. The zircons studied by Mortensen et al. (1992, 1997) had very low Th/U ratios of <0.01. This observation supports our suggestion that Th and Pa may show contrasting behaviour in fluid-rich magmatic systems.

If U-Pb discordance in the Kovdor baddeleyite is related to the excess of ^{231}Pa, it requires ~100-fold increase of ^{231}Pa/^{235}U relative to the melt in secular equilibrium. Considering the extreme Th/U and Nb/Ta fractionation, this level of Pa/U fractionation is not unlikely. Preliminary U-Pb data for baddeleyite from carbonatite of the Guli intrusive-volcanic complex of the Meymecha-Kotui area (Kamo et al. 2000) suggest that discordance related to the presence of excess ^{207}Pb, presumably produced from excess ^{231}Pa, may be a common feature of carbonatitic baddeleyite.

6.5. Rb-Sr vs. U-Th-Pb Age Discrepancy: Is it Caused by Slow Cooling?

The Rb-Sr mica results from two phoscorites and three carbonatites are perfectly internally consistent and define a precise isochron age of 372.2 ± 1.5 Ma, which is 5 to 7 m.y. younger than our best estimate based on ^{206}Pb/^{238}U in baddeleyite, and other reliable U-Th-Pb age values. The initial ^{87}Sr/^{86}Sr ratio of 0.70368 ± 0.00055 from the mica isochron is identical to the Sr isotopic composition measured in low-Rb/Sr calcite and apatite from the same samples (Zaitsev and Bell 1995). Mica grains are very well preserved, with no signs of alteration that might suggest resetting of the Rb-Sr system. The Rb-Sr mica isochron age is therefore expected to reflect the timing of crystallisation, or the timing of closure of the Rb-Sr system.

We first consider the possibility that the Rb-Sr vs. U-Th-Pb age discrepancy is caused by the difference in closure temperature in a slowly cooling system. The closure temperature for Pb diffusion in apatite is ~600°C as discussed above. The estimates for Rb-Sr system in phlogopite and biotite from slowly cooling igneous and metamorphic rocks yielded the range of closure temperatures from 300°C to 400°C (Armstrong et al. 1966, Verschure et al. 1980, Del Moro et al. 1982, Jenkin et al. 2001). Recent experimental determination of diffusion rate of Sr in phlogopite (Hammouda and Cherniak 2000) shows strong heterogeneity of diffusion, and suggests a range of closure temperatures between 400 to 700°C depending on crystallographic direction. The lower closure temperature estimate is consistent with the results from natural systems. For modelling purposes, we assume the closure temperature of 300°C, at the lower limit of the values determined in natural systems.

The question of whether the difference in closure temperatures can be responsible for the ca. 5 to 7 m.y. difference between U-Th-Pb and Rb-Sr ages also depends on the cooling rate of the Kovdor massif. Fortunately, the estimate of the cooling rate for the Kovdor massif is relatively straightforward. The intrusions of the Kola Alkaline Province were emplaced in anorogenic conditions, therefore their cooling was controlled by diffusive heat transfer from the intrusive bodies to a much larger volume of stable and relatively cold host upper crust. Here we consider the cooling scenario, in which all igneous phases of the Kovdor massif were emplaced within a short time, and the entire massif cooled as a single body. This is the case of slowest cooling for late igneous phases, including carbonatites and phoscorites.

The Kovdor massif is a stock (approximately elliptical cylinder) with radii of 3 and 5 km (Kukharenko et al. 1965, Arzamastsev et al. 2000, see also Fig. 1). We assume the length of the cylinder of 20 km, a maximum estimate based on gravity modelling of Arzamastsev et al. (2000). The depth of emplacement for the present erosional level of the Kovdor massif is estimated at 2 to 4 km (Kukharenko et al. 1965, Samoilov and

Bagdasarov 1975). With average continental geothermal gradient of 30°C/km and surface temperature of 0°C, we obtain the temperature of the crust of 60 to 120°C at the level of emplacement. Applying the formalism for cooling stock developed by Lovering (1935), and using the range of possible thermal properties of rocks (Irvine 1970, Clauser and Huenges 1995), we obtain the duration of cooling from 600°C to 300°C at the centre of the body: 332 to 453 thousand years for the case of crustal temperature of 100°C (average geothermal gradient, best estimate of the depth of emplacement), and 671 to 917 thousand years for the case of crustal temperature of 200°C (unusually high geothermal gradient, or emplacement at greater depth). Any reasonable modifications of the model: late emplacement of carbonatites and/or phoscorites, additional heat transfer with magmatic fluids, displacement of carbonatites and phoscorites from the centre of intrusion, or higher closure temperature for Rb-Sr in phlogopite, would result in a higher estimate of the cooling rate.

These estimates show that slow cooling of the Kovdor massif can explain no more than 20% of the observed 5 to 7 m.y. age difference between U-Th-Pb-bearing minerals and Rb-Sr in phlogopite. With most probable model parameters slow cooling accounts for less that 10% of the age difference. We should thus consider other possible causes of this age discrepancy.

6.6. Rb-Sr vs. U-Th-Pb Age Discrepancy: A Manifestation of the Decay Constant Problem?

The low Rb-Sr age is difficult to reconcile with the U-Th-Pb ages without assuming that the decay constant of ($\lambda\ ^{87}$Rb) of $1.42*10^{-11}\ y^{-1}$, recommended by Subcomission on Geochronology (Steiger and Jäger 1977) and used by most of researchers since then, may be incorrect. The recommended ^{87}Rb has not gained unanimous acceptance among geochronologists, and has been contested mainly by researchers studying meteorite and lunar chronology (Minster et al. 1982, Shih et al. 1985) on the basis of comparison between Rb-Sr and U-Pb ages. The evidence for the lower than recommended value of $\lambda\ ^{87}$Rb has been summarised by Begemann et al. (2001). The comparative Rb-Sr and U-Th-Pb data for terrestrial igneous rocks have not been used in re-evaluation of the $\lambda\ ^{87}$Rb value since the early days of geochronology, because the rocks suitable for precise and accurate dating with both Rb-Sr and U-Th-Pb, and satisfying other requirements for accurate cross-calibration, can rarely be found (Begemann et al. 2001). Relatively small (i.e., fast cooling) and well preserved (free of metamorphic overprint) anorogenic alkaline-carbonatite intrusions like the Kovdor massif may be among the favourable exceptions. Assuming that the best baddeleyite age and the mica isochron age both correspond to crystallisation of phoscorites and carbonatites (i.e., ignoring any effects of slow cooling), we obtain $\lambda\ ^{87}\text{Rb} = (1.396 \pm 6)*10^{-11}y^{-1}$ (0.43%, 2σ error), relative to the $\lambda\ ^{238}\text{U} = 1.55125*10^{-10}\ y^{-1}$ (Jaffey et al. 1971). The error is a quadratic sum of the relative errors in the Rb-Sr and U-Pb ages, and the conservative estimate of the uncertainty in ^{238}U of 0.16% after Mattinson (1987, 2000).

The calculated $\lambda\ ^{87}$Rb value will be slightly higher, if the effect of slow cooling is taken into consideration. If the diffusion rates (and thus the closure temperatures) of Pb in apatite and Sr in phlogopite are assumed to be similar, then the comparison between phlogopite Rb-Sr and apatite U-Th-Pb will give accurate $\lambda\ ^{87}$Rb value. Unfortunately the ^{206}Pb/^{238}U system in the Kovdor apatite is obscured with an unknown amount of initial excess ^{230}Th, and the ^{207}Pb/^{235}U chronometer is not sufficiently precise to allow useful comparison. The ^{208}Pb/^{232}Th apatite age is precise and free of initial disequilibrium effect, but the error in $\lambda\ ^{232}\text{Th}=4.948*10^{-11}\ y^{-1}$ (Le Roux and Glendenin 1963) of 1.02% (2σ), adds an unacceptably large uncertainty to the calculated $\lambda\ ^{87}$Rb value. We can, however, use our zircon and baddeleyite U-Pb and Th-Pb data to evaluate $\lambda\ ^{232}$Th relative to the "gold standard" $\lambda\ ^{238}$U more precisely, and use this new $\lambda\ ^{232}$Th value further to calculate $\lambda\ ^{87}$Rb. Assuming that baddeleyite and zircon were formed simultaneously, we obtain $\lambda\ ^{232}\text{Th} = (4.934 \pm 15)*10^{-11}\ y^{-1}$ (0.31%, 2σ error) from ^{206}Pb/^{238}U in the baddeleyite and ^{208}Pb/^{232}Th in the zircon. The recalculated Th-Pb age of apatite with the new $\lambda\ ^{232}$Th is 377.5 Ma, and the $\lambda\ ^{87}$Rb based on comparison between the Th-Pb age of apatite and the Rb-Sr isochron age is $(1.400 \pm 7)*10^{-11}y^{-1}$ (0.53%, 2σ error). If we assume that cooling from the closure temperature of Pb diffusion in apatite to the closure temperature of Sr diffusion in phlogopite took 1 m.y. (a maximum estimate from the thermal modelling), then the calculated $\lambda\ ^{87}$Rb is increased to $1.404*10^{-11}y^{-1}$. Our estimates for $\lambda\ ^{87}$Rb, with or without consideration of slow cooling, are very close to the value of $1.402*10^{-11}\ y^{-1}$ suggested by Minster et al. (1982) and Shih et al. (1985).

6.7. Age of the Kovdor Carbonatites and Phoscorites

With the current precision of dating we have not detected any age differences between the igneous phases within the phoscorites and carbonatites, and suggest that the age of 378.64 Ma applies to the whole body. The age of the geologically earlier and more voluminous phases of ultramafic and alkaline silicate rocks will be explored in a separate study.

7. CONCLUSIONS

Comparative study of multiple geochronometer minerals from the Kovdor phoscorite-carbonatite body revealed an exceptional complexity of isotopic systems, which can be understood though systematic analysis of possible sources of distortion. From these data, we can draw a number of conclusions at two different levels of confidence.

Almost certainly:

1. Determination of precise and accurate age of carbonatites and phoscorites requires study of multiple minerals and multiple isotopic systems No single geochronometer is sufficiently reliable. The Th-Pb geochronometry can be a very useful supplement to U-Pb geochronometry.
2. Baddeleyite may be affected by Pb loss up to a few percent The degree of Pb loss varies between rocks. Baddeleyite fractions not affected by Pb loss can provide very precise and consistent ^{206}Pb/^{238}U ages.
3. Phoscorites and carbonatites of the Kovdor massif were emplaced within a short period of time at 378.64 Ma.
4. Disequilibrium in U decay series can present a serious complication to dating even for Palaeozoic rocks

Probably:

1. U-Pb and Th-Pb chronometers in baddeleyite and high-Th zircon show different mobility of radiogenic Pb U-Pb system is more stable in baddeleyite, and Th-Pb is more stable in zircon. This may be explained if uranium and thorium in baddeleyite and in high-Th zircon occupy distinct structural positions. In contrast, the U-Pb and Th-Pb in apatite behave coherently.
2. Baddeleyite may contain unsupported radiogenic ^{207}Pb, which obscures the $^{207}Pb/^{235}U$ and $^{207}Pb/^{206}Pb$ geochronometers. The possible reason is preferential partitioning of protactinium-231 relative to uranium into growing baddeleyite.
3. Rb-Sr system in phlogopite and tetraferriphlogopite single grains allows precise age determination of carbonatites and phoscorites. The discrepancy between Rb-Sr and U-Th-Pb ages did not result from late closure of Rb-Sr system in phlogopite, but suggests that that the decay constant of ^{87}Rb is close to $1.40*10^{-11}$ y^{-1}, rather than to the recommended value of $1.42*10^{-11}$ y^{-1}.

Acknowledgments—We are grateful to T. Bayanova for providing baddeleyite fractions from the samples 1/84 and 244/76. L. Heaman provided most valuable support and advice during the early stages of this study. An important part of this project was completed at the Geochronological Lab of the Washington University supervised by R. Tucker, whom we would like to thank for the access to analytical facilities and for fruitful discussions. XRD analyses were performed by M. Back. Comments by N. Krasnova and S. Kamo, and reviews by U. Schaltegger, J. Mattinson and anonymous reviewer improved the manuscript. Analytical work at the ROM was supported by the operating funds of the Jack Satterly Geochronology Lab. ANZ acknowledges financial support from INTAS (97 to 0722) and Alexander von Humboldt Stiftung.

Associate editor: S. L. Goldstein

REFERENCES

Amelin Yu. V., Heaman L. M., Verchogliad V. M., and Skobelev V. M. (1994) Geochronological constraints on the emplacement history of an anorthosite-rapakivi granite suite: U-Pb zircon and baddeleyite study of the Korosten complex, Ukraine. *Contrib. Mineral. Petrol.* **116,** 411–9.

Amelin Yu. V., Larin A. M., and Tucker R. D. (1997a) Chronology of multiphase emplacement of the Salmi rapakivi granite-anorthosite complex, Baltic Shield: implications for magmatic evolution. *Contrib. Mineral. Petrol.* **127,** 353–68.

Amelin Yu. V., Ritsk E. Yu., and Neymark L. A. (1997b) Effects of interaction between ultramafic tectonite and mafic magma on Nd-Pb-Sr isotopic systyems in the Neoproterozoic Chaya massiof, Baikal-Muya ophiolite belt. *Earth Planet. Sci. Lett.* **148,** 299–316.

Amelin Y., Li C., and Naldrett A. J. (1999) Geochronology of the Voisey's Bay Intrusion, Labrador, Canada, by precise U-Pb dating of coexisting baddeleyite, zircon, and apatite. *Lithos* **47,** 33–51.

Armstrong R. L., Jäger E., and Eberhardt P. (1966) A comparison of K-Ar and Rb-Sr ages of Alpine biotites. *Earth Planet. Sci. Lett.* **1,** 13–9.

Arzamastsev A. A., Glaznev V. N., Raevsky A. B., and Arzamastseva L. V. (2000) Morphology and internal structure of the Kola Alkaline intrusions, NE Fennoscandian Shield: 3D density modelling and geological implications. *J. Asian Earth Sci.* **18,** 213–28.

Barth S., Oberli F., and Meyer M. (1989) U-Th-Pb systematics of morphologically characterized zircon and allanite: a high-resolution isotopic study of the Alpine Rensen pluton (northern Italy). *Earth Planet. Sci. Lett.* **95,** 235–54.

Barth S., Oberli F., and Meyer M. (1994) Th-Pb versus U-Pb isotope systematics in allanite from co-genetic rhyolite and granodiorite: implications for geochronology. *Earth Planet. Sci. Lett.* **124,** 149–59.

Bayanova T. B., Kirnarski Yu. M., Gannibal L.F., Kosheev O.A., and Balashov Yu. A. (1991) U-Pb dating of baddeleyite from Kovdor carbonatite conplex. *Methods of Isotope Geology*:31. (ed. L. K. Levsky) Institute of Geochemistry and Analytical chemistry of the USSR Academy of Science: St. Petersburg (abstract in Russian).

Bayanova T. B., Kirnarski Yu. M., and Levkovich N. V. (1997) A U-Pb study of baddeleyite from rocks of the Kovdor massif. *Doklady Akademii Nauk* **356,** 509–11 (in Russian).

Begemann F., Ludwig K. R., Lugmair G. W., Min K. W., Nyquist L. E., Patchett P. J., Renne P. R., Shih C.-Y., Villa I., and Walker R. J. (2001) Call for an improved set of decay constants for geochronological use. *Geochim. Cosmochim. Acta* **65,** 111–21.

Bell K. (1998) Radiogenic isotope constraints on relationships between carbonatites and associated silicate rocks—a brief review. *J. Petrol.* **39,** 1987–96.

Bell K. and Simonetti A. (1996) Carbonatite magmatism and plume activity: implications from the Nd, Pb and Sr isotope systematics of Oldoinyo Lengai. *J. Petrol.* **37,** 1321–39.

Bulakh A. G. and Ivanikov V. V. (1984) *Problems of mineralogy and petrology of carbonatites*. Leningrad Univeristy Press: Leningrad (in Russian).

Cherniak D. J. and Watson E. B. (2000) Pb diffusion in zircon. *Chem. Geol.* **172,** 5–24.

Cherniak D. J., Hanchar J. M., and Watson E. B. (1997) Diffusion of tetravalent cations in zircon. *Contrib. Mineral. Petrol.* **127,** 383–90.

Cherniak D. J., Lanford W. A., and Ryerson F. J. (1991) Lead diffusion in apatite and zircon using ion implantation and Rutherford Backscattering techniques. *Geochim. Cosmochim. Acta.* **55,** 1663–73.

Clauser C. and Huenges E. (1995) Thermal conductivity of rocks and minerals. *Rock Physics and Phase Relations: A handbook of Physical Constants* (ed. T. J. Ahrens), 105–126. American Geophysical Union: Washington, DC.

Collerson K. D., MuCulloch M. T., and Nutman A.P. (1989) Sr and Nd isotope systematics of polymetamorphic Archean gneisses from southern West Greenland and northern Labrador. *Can. J. Earth Sci.* **26,** 446–66.

Dauphas N. and Marty B. (1999) Heavy nitrogen in carbonatites of the Kola Peninsiula: a possible signature of the deep mantle. *Science* **286,** 2488–90.

Del Moro A., Puxeddu M., Radicati di Brozolo F., and Villa I.M. (1982) Rb-Sr and K-Ar ages on minerals at temperatures of 300–400°C from deep wells of the Larderello geothermal field (Italy). *Contrib. Mineral. Petrol.* **81,** 340–9.

Dunaev V. A. (1982) Structure of Kovdor ore deposit. *Geol. Ore Dep.* **3,** 28–36 (in Russian).

Edwards R. L., Chen J. H., and Wasserburg G.J. (1986) ^{238}U-^{234}U-^{230}Th-^{232}Th systematics and the precise measurement of time over the past 500,000 years. *Earth Planet. Sci. Lett.* **81,** 175–92.

Evzikova N. Z. (1960) About the preferred oriented growth and the habit change of pyrochlore crystals. *Zapiski Vses. Mineral. Obshchestva.* **89**(5)**,** 555–60.

Friel J. J and Ulmer G. C. (1974) Oxygen fugacity geothermometry of the Oka carbonatite. *Am. Mineral.* **59,** 314–8 (in Russian).

Gerlach D. C., Cliff R. A., Davies G. R., Norry N., and Hodgson N. (1988) Magma sources of the Cape Verdes archipelago: isotopic and trace element constrains. *Geochim. Cosmochim. Acta* **52,** 2979–92.

Hammouda T. and Cherniak D. J. (2000) Diffusion of Sr in fluorphlogopite determined by Rutherford backscattering spectrometry. *Earth Planet. Sci. Lett* **178,** 339–49.

Heaman L. M. and LeCheminant A. N. (1993) Paragenesis and U-Pb systematics of baddeleyite (ZrO_2). *Chem. Geol.* **110,** 95–126.

Heaman L. M., LeCheminant A. N., and Rainbird R. H. (1993) Nature and timing of Franklin igneous events, Canada: Implications for a Late Proterozoic mantle plume and the break-up of Laurentia. *Earth Planet. Sci. Lett.* **109,** 117–31.

Holland H. D. and Gottfried D. (1955) The effect of nuclear radiation on the structure of zircon. *Acta Crystallogr* **8,** 291–300.

Irvine T. N. (1970) Heat transfer during solidification of layered intrusions. 1. Sheets and sills. *Can. J. Earth Sci* **7,** 1031–61.

Jaffey A. H., Flynn K. F., Glendenin L. E., Bentley W. C., and Essling A. M. (1971) Precision measurement of half-lives and specific activities of ^{235}U and.^{238}U. *Phys. Rev. C.* **4**(5)**,** 1889–1906.

Jenkin G. R. T., Ellam R. M., Rogers G., and Stuart F. M. (2001) An investigation of closure temperature of the biotite Rb-St system: The importance of cation exchange. *Geochim. Cosmochim. Acta* **65,** 1141–60.

Jones J. H., Walker D., Pickett D. A., Murrell M. T., and Beattie P. (1995) Experimental investigation of the partitioning of Nb, Mo, Ba, Ce, Pb, Ra, Th, Pa and U between immiscible carbonate and silicate liquids. *Geochim. Cosmochim. Acta.* **59,** 1307–20.

Kamo S. L., Czamanake G. K., Amelin Y., Fedorenko V. A., Trofimov V. R. (2000) U-Pb zircon and baddeleyite and U-Th-Pb perovskite ages for Siberian flood basalt volcanism. *Tenth International V.M. Goldschmidt Conference, Oxford, UK. Journal of Conference Abstracts* **5(2),** 569.

Kapustin Yu. L. (1980) *Mineralogy of carbonatites*. Amerind Publishing: New Delhi.

Karpenko M. I., Ivanenko V. V. (1994) ^{39}Ar-^{40}Ar data on excessive., ^{40}Ar in nepheline from the Kovdor massif: Kola Peninsula. *Eighth Int. Conf. Geochron. Cosmochron. Isot. Geol., USGS Circular* **1107 124.**.

Kramm U. (1993) Mantle components of carbonatites from the Kola Alkaline Province, Russia and Finland: a Nd-Sr study. *Eur. J. Mineral.* **5,** 985–9.

Kramm U., Kogarko L. N., Kononova V. A., and Vartiainen H. (1993) The Kola Alkaline Province of the CIS and Finland: precise Rb-Sr ages define 380–360 Ma range for all magmatism. *Lithos* **30,** 33–4.

Krasnova N. I. and Kopylova L. N. (1988) The geologic basis for mineral-technological mapping at the Kovdor ore deposit. *Int. Geol. Review.* **30,** 307–19.

Krasnova N. I., Kartenko N. F., Rimskaya-Korsakova O. M., Firyulina V. V. (1967) Thorianite from the phlogopite-bearing rocks of Kovdor massif. In *Mineralogy and Geochemistry*. **No 2.** pp. 19&27. Leningrad State University Press. (In Russian).

Krogh T. E. (1973) A low-contamination method for hydrothermal decomposition of zircon and extraction of U and Pb for isotope age determinations. *Geochim. Cosmochim. Acta* **37,** 485–94.

Krogh T. E. (1982) Improved accuracy of U-Pb zircon ages using an air abrasion technique. *Geochim. Cosmochim. Acta* **46,** 637–49.

Krogstad E. J. and Walker R. J. (1994) High closure temperatures of the U-Pb system in large apatites from the Tin Mountain pegmatite, Black Hills, South Dacota, USA. *Geochim. Cosmochim. Acta* **58,** 3845–53.

Kukharenko A.A., Orlova M. P., Boulakh A. G., Bagdasarov E. A., Rimskaya-Korsakova O. M., Nefedov E. L., Ilinsky G. A., Sergeev A. S., Abakumova L. B. (1965) The Caledonian complexes of ultrabasic-alkaline and carbonatite rocks on Kola penimsula and in Northern Karlia (geology, petrology, mineralogy and geochemistry). Nedra, Moscow (in Russian): Nedra.

Le Roux L. J. and Glendenin L. E. (1963) Half-life of thorium-232. *Nat. Conf. Nuclear Energy Appl. Isotop Radiat. Proc.* 77–88.

Lee J. K., Williams I. S., and Ellis D. J. (1997) Pb, U and Th diffusion in natural zircon. *Nature* **390,** 159–62.

Lovering T. S. (1935) Theory of heat conduction applied to geological problems. *Bull. Geol. Soc. Am.* **46,** 69–94.

Ludwig K. R. (1977) Effect of initial radioactive-daughter disequilibrium on U-Pb isotope apparent ages of young minerals. *J. Res. U. S. G. S.* **5,** 663–7.

Ludwig K. R. (1997) ISOPLOT: A plotting and regression program for radiogenic-isotope data; Version 2.95.*USGS Open-File Report* 91–445 (July 1997 rev.).

Ludwig K. R. (1993) PBDAT. A computer program for processing Pb-U-Th data version 1.24, US Geological Survey Open-file Report 88–542, Revision of June 22, 1993, 34 pp.

Ludwig K. R. (1998) On the treatment of concordant uranium-lead ages. *Geochim. Cosmochim. Acta* **62,** 665–76.

Ludwig K. R. (2000) Decay constant errors in U-Pb concordia-intercept ages. *Chem. Geol* **166,** 315–8.

Marty B., Tolstikhin I., Kamensky I. L., Nivin V., Balaganskaya E., and Zimmermann J.-L. (1998) Plume-derived rare gases in 380 Ma carbonatites from the Kola region (Russia) and the argon isotopic composition in the deep mantle. *Earth Planet. Sci. Lett.* **164,** 179–92.

Mattinson J. M. (1973) Anomalous isotopic composition of lead in young zircons. *Carnegie Inst. Wash. Yrbk.* **72,** 613–616.

Mattinson J. M. (1987) U-Pb ages of zircons: a basic examination of error propagation. *Chem. Geol.* **66,** 151–62.

Mattinson J. M. (2000) Revising the"Gold Standard"—the uranium decay constant of Jaffey et al.,1971 AGU Spring Meeting.

Minster J-F., Birck J.-L., and Allègre C. J. (1982) Absolute age of formation of chondrites studied by the ^{87}Rb-^{87}Sr method. *Nature* **300,** 414–9.

Mortensen J. K., Roddick J. C., and Parrish R. R. (1992) Evidence for high levels of unsupported ^{207}Pb in zircon from a granitic pegmatite: Implications for interpretation of discordant U-Pb data. *EOS, Trans., Am. Geophys. Union.* **73**(14)**,** 370.

Mortensen J. K., Williams I. S., and Compston W. (1997) Ion microprobe and cathodoluminescence investigations of unsupported ^{207}Pb. *GAC-MAC Ann. meeting, Abstr.* **Vol. 22,** A-105.

Neymark L. A., Amelin Y., and Paces J. B. (2000) ^{206}Pb-^{230}Th-^{234}U-^{238}U and ^{207}Pb-^{235}U geochronoloy of Quaternary opal, Yucca Mountain, Nevada. *Geochim. Cosmochim. Acta* **64,** 2913–28.

Papanastassiou D. A. and Wasserburg G. J. (1971) Rb-Sr ages of igneous rocks from the Appllo 14 mission and the age of the Fra Mauro formation. *Earth Planet. Sci. Lett.* **12,** 36–48.

Pyle D. M., Dawson J. B., and Ivanovich M. (1991) Short-lived decay series disequilibria in the natrocarbonatite lavas of Oldoinyo Lengai, Tanzania: constraints on the timing of magma genesis. *Earth Planet. Sci. Lett.* **105,** 378–96.

Samoylov V. S. and Bagdasarov Y. A. (1975) Depth facies of carbonatites and associated rocks. *Izvestiya Akademii Nauk SSSR, Seriya Geologicheskaya* **10,** 27–35 (in Russian).

Schärer U. (1984) The effect of initial ^{230}Th disequilibrium on young U-Pb ages: the Makalu case, Himalaya. *Earth Planet. Sci. Lett.* **67,** 191–204.

Shih C.-Y., Nyquist L. E., Bogard D. D., Wooden J. L., Bansal B. M., and Wiesmann H. (1985) Chronology and petrogenesis of a 1.8g lunar granitic clast: 14321, 1062. *Geochim. Cosmochim. Acta* **49,** 411–26.

Steiger R. and Wasserburg G. J. (1966) Systematics in the Pb ^{208}-Th ^{232}, Pb ^{207}-U ^{235}, and Pb ^{206}-U ^{238} systems. *J. Geophys. Res.* **71,** 6065–90.

Steiger R. H. and Jäger E. (1977) Subcommission on geochronology: convention on the use of decay constants in geo- and cosmochronology. *Earth Planet. Sci. Lett.* **36,** 359–62.

Tatsumoto M. (1966) Isotopic composition of lead in volcanic rocks from Hawaii, Iwo Jima, and Japan. *J. Geophys. Res.* **71,** 1721–33.

Ternovoi V. I. (1977) Carbonatite Complexes and their ore deposits. Leningrad State University Press, Leningrad, 169 pp. (in Russian).

Treiman A. H. and Essene E. J. (1984) A periclase-dolomite-calcite carbonatite from the Oka complex, Quebec, and its calculated volatile composition. *Contrib. Mineral. Petrol.* **85,** 149–57.

Veksler I. V., Nielsen T. F. D., and Sokolov S. V. (1998a) Mineralogy of crystallized inclusions from Gardiner and Kovdor ultramafic alkaline complexes: implications for carbonatite genesis. *J. Petrol.* **39,** 2015–31.

Veksler I. V., Petibon C., Jenner G. A., Dorfman A. M., and Dingwell D. B. (1998b) Trace element partitioning in immiscible silicate-carbonate liquid systems: An initial experimental study using a centrifuge autoclave. *J. Petrol.* **39,** 2095–104.

Velhurst A., Balaganskaya E., Kirnarsky Y., and Demaiffe D. (2000) Petrological and geochemocal (trace elements and Sr-Nd isotopes) characteristics of the Paleozoic Kovdor ultramafic, alkaline and carbonatite intrusion (Kola Peninsula, Russia). *Lithos* **51,** 1–25.

Verschure R. H., Andriessen P. A. M., Boelrijk N. A. I. M., Hebeda E. H., Maijer C., Priem H. N. A., and Verdurmen E. A. T. (1980) On the thermal stability of Rb-Sr and K-Ar biotite systems: evidence from coexisting Sveconorwegian (ca 870 Ma) and Caledonian (ca 400 Ma) biotites in SW Norway. *Contrib. Mineral. Petrol.* **74,** 245–52.

Walter H. J., Rutgers van der Loeff M. M., and Hoeltzen H. (1997) Enhanced scavenging of ^{231}Pa relative to ^{230}Th in the South Atlantic south of the Polar Front: Implications for the use of the

$^{231}Pa/^{230}Th$ as a paleoproductivity ratio. *Earth Planet. Sci. Lett.* **149,** 85–100.

Watson E. B., Harrison T. M., and Ryerson F. J. (1985) Diffusion of Sm, Sr, and Pb in fluorapatite. *Geochim. Cosmochim. Acta* **49,** 1813–23.

Wiedenbeck M., Allé P., Corfu F., Griffin W. L., Meier M., Oberli F., von Quadt A., Roddick J. C., and Spiegel W. (1995) Three natural zircon standards for U-Th-Pb, Lu-Hf, trace element and REE analyses. *Geostand. Newsl.* **19,** 1–23.

Williams C. T. (1996) The occurrence of niobian zirconolite, pyrochlore and baddeleyite in the Kovdor carbonatite complex, Kola Peninsula, Russia. *Mineral. Mag.* **60,** 639–46.

Williams R. W., Gill J. B., and Bruland D. W. (1986) Ra-Th disequilibria systematics: timescale of carbonatite magma formation at OldoinyoLengai volcano, Tanzania. *Geochim. Cosmochim. Acta* **50,** 1249–59.

Zaitsev A. and Bell K. (1995) Sr and Nd isotope data of apatite, calcite and dolomite as indicators of source, and the relationships of phoscorites and carbonatites from the Kovdor massif, Kola peninsula, Russia. *Contrib. Mineral. Petrol.* **121,** 324–35.